

# Correspondence

## 1 Compressive-Sensing-Based Multiuser Detector for the 2 Large-Scale SM-MIMO Uplink

3 Zhen Gao, Linglong Dai, Zhaocheng Wang, *Senior Member, IEEE*,  
4 Sheng Chen, *Fellow, IEEE*, and Lajos Hanzo, *Fellow, IEEE*

5 **Abstract**—Conventional spatial modulation (SM) is typically consid-  
6 ered for transmission in the downlink of small-scale multiple-input-  
7 multiple-output (MIMO) systems, where a single antenna element (AE) of  
8 a set of, e.g.,  $2^P$  AEs is activated for implicitly conveying  $p$  bits. By contrast,  
9 inspired by the compelling benefits of large-scale MIMO (LS-MIMO)  
10 systems, here, we propose an LS-SM-MIMO scheme for the uplink (UL),  
11 where each user having multiple AEs but only a single radio frequency  
12 (RF) chain invokes SM for increasing the UL throughput. At the same time,  
13 by relying on hundreds of AEs and a small number of RF chains, the base  
14 station (BS) can simultaneously serve multiple users while reducing the  
15 power consumption. Due to the large number of AEs of the UL users and  
16 the comparably small number of RF chains at the BS, the UL multiuser sig-  
17 nal detection becomes a challenging large-scale underdetermined problem.  
18 To solve this problem, we propose a joint SM transmission scheme and  
19 a carefully designed structured compressive sensing (SCS)-based multi-  
20 user detector (MUD) to be used at the users and the BS, respectively.  
21 Additionally, the cyclic-prefix single carrier (CPSC) is used to combat  
22 the multipath channels, and a simple receive AE selection is used for the  
23 improved performance over correlated Rayleigh-fading MIMO channels.  
24 We demonstrate that the aggregate SM signal consisting of multiple UL  
25 users' SM signals of a CPSC block exhibits distributed sparsity. Moreover,  
26 due to the joint SM transmission scheme, aggregate SM signals in the same  
27 transmission group exhibit group sparsity. By exploiting these intrinsically  
28 sparse features, the proposed SCS-based MUD can reliably detect the  
29 resultant SM signals with low complexity. Simulation results demonstrate  
30 that the proposed SCS-based MUD achieves a better signal detection  
31 performance than its counterparts even with higher UL throughput.

32 **Index Terms**—Compressive sensing (CS), large-scale multiple-input-  
33 multiple-output (LS-MIMO), multiuser detector (MUD), spatial modula-  
34 tion (SM).

### 35 I. INTRODUCTION

36 A widely recognized consensus is that fifth-generation (5G) sys-  
37 tems will be capable of providing significant energy efficiency and  
38 system capacity improvements [1], [2]. Promising techniques, such  
39 as large-scale multiple-input-multiple-output (LS-MIMO) and spatial  
40 modulation (SM)-MIMO systems, are considered as potent candidates  
41 for 5G systems [1]–[5]. LS-MIMO employing hundreds of antenna

elements (AEs) at the base station (BS) is capable of improving 42  
spectral efficiency by orders of magnitude, but it suffers from the 43  
nonnegligible power consumption and hardware cost due to one spe- 44  
cific radio frequency (RF) chain usually required by every AE [5]. 45  
By using a reduced number of RF chains, the emerging SM-MIMO 46  
activates part of available AEs to transmit extra information in the 47  
spatial domain, and it has attracted much attention due to its high en- 48  
ergy efficiency and reduced hardware cost [5]. However, conventional 49  
SM-MIMO is usually considered in the downlink of small-scale 50  
MIMO systems, and therefore, its achievable capacity is limited. Indi- 51  
vidually, both technologies have their own advantages and drawbacks. 52  
By an effective combination of them, one can envision the win-win 53  
situation. SM-MIMO is attractive for LS-MIMO systems, since the 54  
reduced number of required RF chains in SM-MIMO can reduce the 55  
power consumption and hardware cost in conventional LS-MIMO 56  
systems. Moreover, hundreds of AEs used in LS-MIMO can im- 57  
prove the system throughput of SM-MIMO. Such reciprocity enables 58  
LS-MIMO and SM-MIMO to enjoy the apparent compatibility. 59

In this paper, we propose an LS-SM-MIMO scheme for intrinsi- 60  
cally amalgamating the compelling benefits of both LS-MIMO and 61  
SM-MIMO for the 5G uplink (UL) over frequency-selective fading 62  
channels. In the proposed scheme, each UL user equipped with mul- 63  
tiple AEs but only a single RF chain invokes SM for increasing the 64  
UL throughput, and the cyclic-prefix single-carrier (CPSC) transmis- 65  
sion scheme is adopted to combat the multipath channels [6]. At the 66  
BS, hundreds of AEs but only dozens of RF chains are employed to 67  
simultaneously serve multiple users, and a direct AE selection scheme 68  
is used to improve the system performance over correlated Rayleigh- 69  
fading MIMO channels at the BS [7]. The proposed scheme can 70  
be adopted in conventional LS-MIMO as a specific UL-transmission 71  
mode for reducing the power consumption or, alternatively, for energy- 72  
and cost-efficient LS-SM-MIMO, where joint benefits of efficient AE 73  
selection [7], transmit precoding [8], and channel estimation [9] can 74  
be readily exploited. To sum up, the proposed scheme inherits the 75  
advantages of LS-MIMO and SM-MIMO, while reducing the power 76  
consumption and hardware cost. 77

A challenging problem in the proposed UL LS-SM-MIMO scheme 78  
is how to realize a reliable multiuser detector (MUD) with low com- 79  
plexity. The optimal maximum likelihood (ML) signal detector suffers 80  
from excessive complexity. Conventional sphere decoding detectors 81  
cannot be readily used in multiuser scenarios and may still exhibit high 82  
complexity for LS-SM-MIMO [10]. Existing low-complexity linear 83  
signal detectors, e.g., the minimum mean square error (MMSE)-based 84  
signal detector, perform well for conventional LS-MIMO systems 85  
[4]. However, they are unsuitable for the proposed LS-SM-MIMO 86  
UL transmission, since the large number of transmit AEs of the UL 87  
users and the reduced number of receive RF chains at the BS make 88  
UL multiuser signal detection a large-scale underdetermined/rank- 89  
deficient problem. The authors in [11]–[13] proposed compressive 90  
sensing (CS)-based signal detectors to solve the underdetermined 91  
signal detection problem in SM-MIMO systems, but they only consid- 92  
ered the single-user small-scale SM-MIMO systems in the downlink. 93

Against this background, our new contribution is that we exploit 94  
the specific signal structure in the proposed multiuser LS-SM-MIMO 95  
UL transmission, where each user only activates a single AE in each 96  
time slot. Hence, the SM signal of each UL user is sparse with 97

Manuscript received May 7, 2015; revised October 1, 2015; accepted  
November 14, 2015. This work was supported in part by the Interna-  
tional Science and Technology Cooperation Program of China under Grant  
2015DFG12760, by the National Natural Science Foundation of China under  
Grant 61571270 and Grant 61201185, by the Beijing Natural Science Founda-  
tion under Grant 4142027, and by the Foundation of Shenzhen government.  
The review of this paper was coordinated by Dr. Y. Xin.

Z. Gao, L. Dai, and Z. Wang are with the Tsinghua National Laboratory for  
Information Science and Technology (TNList), Department of Electronic Engi-  
neering, Tsinghua University, Beijing 100084, China (e-mail: gao-z11@mails.  
tsinghua.edu.cn; daill@mail.tsinghua.edu.cn; zcwang@mail.tsinghua.edu.cn).

S. Chen and L. Hanzo are with the School of Electronics and Computer  
Science, University of Southampton, Southampton SO17 1BJ, U.K. (e-mail:  
sqc@ecs.soton.ac.uk; lh@ecs.soton.ac.uk).

Color versions of one or more of the figures in this paper are available online  
at <http://ieeexplore.ieee.org>.

Digital Object Identifier 10.1109/TVT.2015.2501460

98 the sparsity level of one, and the aggregate SM signal consisting  
 99 of multiple UL users' SM signals of a CPSC block exhibits certain  
 100 distributed sparsity, which can be beneficially exploited for improving  
 101 the signal detection performance at the BS. Moreover, we propose  
 102 a joint SM transmission scheme for the UL users in conjunction  
 103 with an appropriately structured CS (SCS)-based MUD at the BS.  
 104 The proposed SCS-based MUD is specifically tailored to leverage  
 105 the inherently distributed sparsity of the aggregate SM signal and the  
 106 group sparsity of multiple aggregate SM signals, owing to the joint SM  
 107 transmission scheme for reliable signal detection performance. Our  
 108 simulation results demonstrate that the proposed SCS-based MUD is  
 109 capable of outperforming the conventional detectors even with higher  
 110 UL throughput.

111 The rest of this paper is organized as follows. Section II introduces  
 112 the system model of the proposed LS-SM-MIMO scheme. Section III  
 113 specifies the proposed joint SM transmission and SCS-based MUD.  
 114 Section IV provides our simulation results. Section V concludes this  
 115 paper.

116 Throughout this paper, lowercase and uppercase boldface letters  
 117 denote vectors and matrices, respectively, whereas  $(\cdot)^T$ ,  $(\cdot)^*$ ,  $(\cdot)^\dagger$ , and  
 118  $[\cdot]$  denote the transpose, conjugate transpose, Moore–Penrose matrix  
 119 inversion, and the integer floor operators, respectively. The  $l_0$  and  
 120  $l_2$  norm operations are given by  $\|\cdot\|_0$  and  $\|\cdot\|_2$ , respectively. The  
 121 support set of vector  $\mathbf{x}$  is denoted by  $\text{supp}\{\mathbf{x}\}$ , and  $\mathbf{x}_i$  denotes the  $i$ th  
 122 entry of vector  $\mathbf{x}$ . Additionally,  $\mathbf{x}|_\Gamma$  denotes the entries of  $\mathbf{x}$  defined  
 123 in the set  $\Gamma$ ,  $\Phi|_\Gamma$  denotes the submatrix whose columns comprise the  
 124 columns of  $\Phi$  that are defined in  $\Gamma$ , and  $\Phi_\Gamma$  denotes the submatrix  
 125 whose rows comprise the rows of  $\Phi$  that are defined in  $\Gamma$ . The  
 126 expectation operator is given by  $E\{\cdot\}$ .  $\text{mod}(x, y) = x - \lfloor x/y \rfloor y$  if  
 127  $y \neq 0$  and  $x - \lfloor x/y \rfloor y \neq 0$ , whereas  $\text{mod}(x, y) = y$  if  $y \neq 0$  and  
 128  $x - \lfloor x/y \rfloor y = 0$ .

## 129 II. SYSTEM MODEL

130 We first introduce the proposed LS-SM-MIMO scheme and then  
 131 focus our attention on the UL transmission with an emphasis on the  
 132 multiuser signal detection.

### 133 A. Proposed Multiuser LS-SM-MIMO Scheme

134 As shown in Fig. 1, we consider the proposed LS-SM-MIMO from  
 135 both the BS side and the user side. For conventional LS-MIMO, the  
 136 number of AEs employed by the BS is equal to the number of its RF  
 137 chains [4]. However, the BS in LS-SM-MIMO, as shown in Fig. 1,  
 138 is equipped with a much smaller number of RF chains  $M_{\text{RF}}$  than  
 139 the total number of AEs  $M$ , i.e., we have  $M_{\text{RF}} \ll M$ . Conventional  
 140 LS-MIMO systems typically assume single-antenna users [4]. By  
 141 contrast, in the proposed scheme, each user is equipped with  $n_t > 1$   
 142 AEs but only a single RF chain, and SM is adopted for the UL  
 143 transmission, where only one of the available AEs is activated for  
 144 data transmission. It has been shown that the main power consumption  
 145 and hardware cost of cellular networks comes from the radio access  
 146 network [1]. Hence, using a reduced number of expensive RF chains  
 147 compared with the total number of AEs at the BS can substantially  
 148 reduce both the power consumption and the hardware cost for the  
 149 operators. Meanwhile, it is feasible to incorporate several AEs and a  
 150 single RF chain in the handsets. The resultant increased degrees of  
 151 freedom in the spatial domain may then be exploited for improving  
 152 the UL throughput. The proposed scheme can be considered as an  
 153 optional UL-transmission mode in conventional LS-MIMO systems,  
 154 where AE selection schemes may be adopted for beneficially selecting  
 155 the most suitable  $M_{\text{RF}}$  AEs at the BS to receive UL SM signals [7].  
 156 Alternatively, it can also be used for the UL of LS-SM-MIMO, when

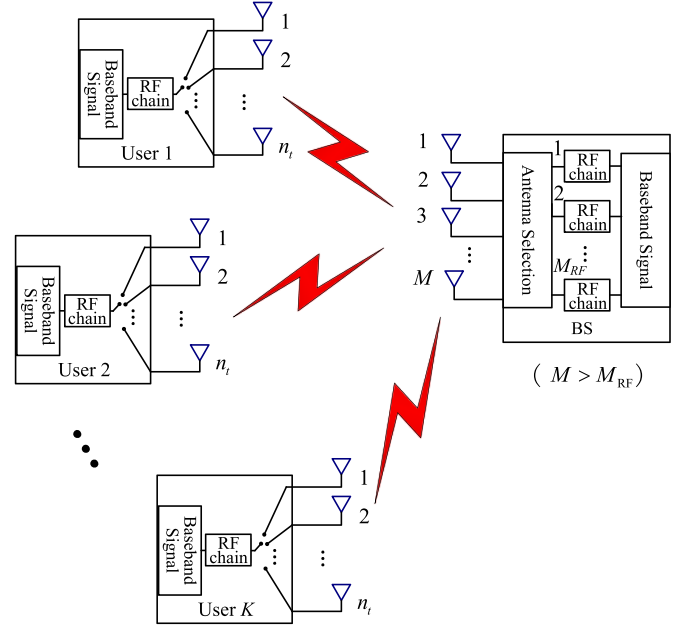


Fig. 1. In the proposed UL LS-SM-MIMO, the BS is equipped with  $M$  AEs and  $M_{\text{RF}}$  RF chains to simultaneously serve  $K$  users, where  $M \gg M_{\text{RF}} > K$ , and each user is equipped with  $n_t > 1$  AEs and one RF chain. By exploiting the improved degree of freedom in the spatial domain, multiple users can simultaneously exploit SM for improving the UL throughput.

157 advantageously combining transmit precoding, receive AE selection,  
 158 and channel estimation [7]–[9].

### 159 B. Uplink Multiuser Transmission

We first consider the generation of SM signals at the users. The SM  
 160 signal  $\mathbf{x}_k = \mathbf{e}_k s_k$  transmitted by the  $k$ th user in a time slot consists  
 161 of two parts: the spatial constellation symbol  $\mathbf{e}_k \in \mathbb{C}^{n_t}$  and the signal  
 162 constellation symbol  $s_k \in \mathbb{C}$ .  $\mathbf{e}_k$  is generated by mapping  $\lfloor \log_2(n_t) \rfloor$   
 163 bits to the index of the active AE, and typically, the user terminal  
 164 employs  $n_t = 2^p$  AEs, where  $p$  is a positive integer. Due to only a  
 165 single RF chain employed at each user, only one entry of  $\mathbf{e}_k$  associated  
 166 with the active AE is equal to one, and the rest of the entries of  $\mathbf{e}_k$  are  
 167 zeros, i.e., we have  
 168

$$\text{supp}(\mathbf{e}_k) \in \mathbb{A}, \quad \|\mathbf{e}_k\|_0 = 1, \quad \|\mathbf{e}_k\|_2 = 1 \quad (1)$$

where  $\mathbb{A} = \{1, 2, \dots, n_t\}$  is the spatial constellation symbol set. The  
 169 signal constellation symbol comes from  $L$ -ary modulation, i.e.,  $s_k \in \mathbb{L}$ ,  
 170 where  $\mathbb{L}$  is the signal constellation symbol set [e.g., 64 quadrature  
 171 amplitude modulation (QAM)] of size  $L$ . Hence, each UL user's SM  
 172 signal carries the information of  $\log_2(L) + \log_2(n_t)$  bits per channel  
 173 use (bpcu), and the overall UL throughput is  $K(\log_2(L) + \log_2(n_t))$   
 174 bpcu. The users rely on the CPSC scheme for transmitting their SM  
 175 signals [6]. Explicitly, each CPSC block consists of a cyclic prefix  
 176 (CP) having the length of  $P - 1$  and the associated data block having  
 177 the length of  $Q$ . Hence, the length of each CPSC block is  $Q + P - 1$ ,  
 178 where this CP is capable of counteracting a dispersive multipath  
 179 channel imposing dispersion over  $P$  samples. The concatenated data  
 180 block consists of  $Q$  successive SM signals.  
 181

At the receiver, due to the reduced number of RF chains at the BS,  
 182 only  $M_{\text{RF}}$  receive AEs can be exploited to receive signals, where exist-  
 183 ing receive AE selection schemes can be adopted to preselect  $M_{\text{RF}}$  re-  
 184 ceive AEs for achieving an improved signal detection performance [7].  
 185 Since the BS can serve  $K$  users simultaneously, after the removal of 186

187 the CP, the received signal  $\mathbf{y}_q \in \mathbb{C}^{M_{\text{RF}}}$  for  $1 \leq q \leq Q$  of the  $q$ th time  
188 slot of a specific CPSC block can be expressed as

$$\begin{aligned} \mathbf{y}_q &= \sum_{k=1}^K \mathbf{y}_{k,q} + \mathbf{w}_q = \sum_{p=0}^{P-1} \sum_{k=1}^K \mathbf{H}_{k,p} \Theta \mathbf{x}_{k, \text{mod}(q-p,Q)} \\ &+ \mathbf{w}_q = \sum_{p=0}^{P-1} \sum_{k=1}^K \tilde{\mathbf{H}}_{k,p} \mathbf{x}_{k, \text{mod}(q-p,Q)} + \mathbf{w}_q \quad (2) \end{aligned}$$

189 where  $\mathbf{H}_{k,p} \in \mathbb{C}^{M \times n_t}$  is the  $k$ th user's MIMO channel matrix for the  
190  $p$ th multipath component, i.e.,  $\mathbf{H}_{k,p} \Theta = \tilde{\mathbf{H}}_{k,p} \in \mathbb{C}^{M_{\text{RF}} \times n_t}$ ; the set  
191  $\Theta$  is determined by the AE selection scheme used; the elements of  
192  $\Theta$  having the cardinality of  $M_{\text{RF}}$  are uniquely selected from the set  
193  $\{1, 2, \dots, M\}$ ;  $\mathbf{x}_{k,q}$  has one nonzero entry; and  $\mathbf{w}_q \in \mathbb{C}^{M_{\text{RF}}}$  is the  
194 additive white Gaussian noise (AWGN) vector with entries obeying  
195 the independent and identically distributed (i.i.d.) circularly symmet-  
196 ric complex Gaussian distribution with zero mean and a variance  
197 of  $\sigma_w^2/2$  per dimension, which is denoted by  $\mathcal{CN}(0, \sigma_w^2)$ .  $\mathbf{H}_{k,p} =$   
198  $\mathbf{R}_{\text{BS}}^{1/2} \tilde{\mathbf{H}}_{k,p} \mathbf{R}_{\text{US}}^{1/2}$ , the entries of  $\tilde{\mathbf{H}}_{k,p}$  obey the i.i.d.  $\mathcal{CN}(0, 1)$ , and  
199  $\mathbf{R}_{\text{US}}$  with the correlation coefficient  $\rho_{\text{US}}$  and  $\mathbf{R}_{\text{BS}}$  with the correlation  
200 coefficient  $\rho_{\text{BS}}$  are correlation matrices at the users and the BS,  
201 respectively. The specific element of the  $m$ th row and the  $n$ th column  
202 of  $\mathbf{R}_{\text{BS}}$  ( $\mathbf{R}_{\text{US}}$ ) is  $\rho_{\text{BS}}^{|m-n|}$  ( $\rho_{\text{US}}^{|m-n|}$ ). For correlated Rayleigh-fading  
203 MIMO channels, the specific  $\Theta$  or receive AE selection scheme has  
204 an impact on the attainable system performance. In this paper, the  
205 direct AE selection scheme is used for maximizing the minimum  
206 geometric distance between any pair of the selected AEs [7]. For  
207 uniform linear arrays (ULAs),  $\Theta = \{\varphi + m_{\text{RF}} \lfloor M/M_{\text{RF}} \rfloor\}_{m_{\text{RF}}=0}^{M_{\text{RF}}-1}$   
208 with  $1 \leq \varphi \leq \lfloor M/M_{\text{RF}} \rfloor - 1$ . Then, (2) can be further expressed as

$$\mathbf{y}_q = \sum_{p=0}^{P-1} \tilde{\mathbf{H}}_p \mathbf{x}_{\text{mod}(q-p,Q)} + \mathbf{w}_q \quad (3)$$

209 by defining  $\tilde{\mathbf{H}}_p = [\tilde{\mathbf{H}}_{1,p}, \tilde{\mathbf{H}}_{2,p}, \dots, \tilde{\mathbf{H}}_{K,p}] \in \mathbb{C}^{M_{\text{RF}} \times (n_t K)}$  and  
210  $\mathbf{x}_q = [(\mathbf{x}_{1,q})^T, (\mathbf{x}_{2,q})^T, \dots, (\mathbf{x}_{K,q})^T]^T \in \mathbb{C}^{(n_t K)}$ . By considering  
211 the  $Q$  SM signals of a specific CPSC block, we arrive at

$$\mathbf{y} = \tilde{\mathbf{H}} \mathbf{x} + \mathbf{w} \quad (4)$$

212 where  $\mathbf{y} = [(\mathbf{y}_1)^T, (\mathbf{y}_2)^T, \dots, (\mathbf{y}_Q)^T]^T \in \mathbb{C}^{(M_{\text{RF}} Q)}$ , the aggregate  
213 SM signal  $\mathbf{x} = [(\mathbf{x}_1)^T, (\mathbf{x}_2)^T, \dots, (\mathbf{x}_Q)^T]^T \in \mathbb{C}^{(K n_t Q)}$ ,  $\mathbf{w} =$   
214  $[(\mathbf{w}_1)^T, (\mathbf{w}_2)^T, \dots, (\mathbf{w}_Q)^T]^T$ , and

$$\tilde{\mathbf{H}} = \begin{bmatrix} \tilde{\mathbf{H}}_0 & \mathbf{0} & \mathbf{0} & \cdots & \tilde{\mathbf{H}}_2 & \tilde{\mathbf{H}}_1 \\ \tilde{\mathbf{H}}_1 & \tilde{\mathbf{H}}_0 & \mathbf{0} & \cdots & \vdots & \tilde{\mathbf{H}}_2 \\ \vdots & \tilde{\mathbf{H}}_1 & \tilde{\mathbf{H}}_0 & \cdots & \tilde{\mathbf{H}}_{P-1} & \vdots \\ \tilde{\mathbf{H}}_{P-1} & \vdots & \tilde{\mathbf{H}}_1 & \cdots & \mathbf{0} & \tilde{\mathbf{H}}_{P-1} \\ \mathbf{0} & \tilde{\mathbf{H}}_{P-1} & \vdots & \vdots & \vdots & \mathbf{0} \\ \vdots & \mathbf{0} & \tilde{\mathbf{H}}_{P-1} & \vdots & \vdots & \vdots \\ \vdots & \vdots & \mathbf{0} & \vdots & \mathbf{0} & \vdots \\ \vdots & \vdots & \vdots & \vdots & \tilde{\mathbf{H}}_0 & \mathbf{0} \\ \mathbf{0} & \mathbf{0} & \mathbf{0} & \cdots & \tilde{\mathbf{H}}_1 & \tilde{\mathbf{H}}_0 \end{bmatrix}. \quad (5)$$

215 The signal-to-noise ratio (SNR) at the receiver is defined by  $\text{SNR} =$   
216  $E\{\|\tilde{\mathbf{H}} \mathbf{x}\|_2^2\} / E\{\|\mathbf{w}\|_2^2\}$ .

The optimal signal detector for (4) relies on the ML algorithm, i.e., 217

$$\begin{aligned} \min_{\tilde{\mathbf{x}}} \|\mathbf{y} - \tilde{\mathbf{H}} \tilde{\mathbf{x}}\|_2 &= \min_{\{\tilde{\mathbf{x}}_{k,q}\}_{k=1,q=1}^{K,Q}} \|\mathbf{y} - \tilde{\mathbf{H}} \tilde{\mathbf{x}}\|_2 \\ \text{s.t. } \text{supp}(\tilde{\mathbf{x}}_{k,q}) &\in \mathbb{A}, \tilde{\mathbf{x}}_{k,q} \in \mathbb{L}, 1 \leq k \leq K, 1 \leq q \leq Q \quad (6) \end{aligned}$$

whose complexity exponentially increases with the number of users, 218  
since the size of the search set for the ML detector is  $(n_t \cdot L)^{KQ}$ . 219  
This excessive complexity can be unaffordable in practice. To reduce 220  
the complexity, near-optimal sphere decoding detectors have been 221  
proposed [10], but their complexity may still remain high, particularly 222  
for the systems supporting large  $K$ ,  $Q$ ,  $n_t$ , and  $L$  [11]. In conventional 223  
LS-MIMO systems, low-complexity linear signal detectors (e.g., the 224  
MMSE-based signal detector) have been shown to be near optimal 225  
since  $M = M_{\text{RF}} \gg K$  and  $n_t = 1$  make multiuser signal detection 226  
an *overdetermined* problem [4]. However, in the proposed scheme, we 227  
have  $M_{\text{RF}} < K n_t$ . Hence, the multiuser signal detection problem (6) 228  
represents a large-scale *underdetermined* problem. Consequently, the 229  
conventional linear signal detectors perform poorly in the proposed 230  
LS-SM-MIMO [11]. By exploiting the sparsity of SM signals, the 231  
authors in [11]–[13] have proposed the concept of CS-based signal 232  
detectors for the downlink of small-scale SM-MIMO operating in a 233  
single-user scenario. However, these signal detectors are unsuitable 234  
for the proposed multiuser scenarios. Observe from (1) that  $\mathbf{x}_{k,q}$  is 235  
a sparse signal having a sparsity level of one. Hence, the aggregate 236  
SM signal  $\mathbf{x}$ , which consists of multiple users' SM signals in  $Q$  237  
time slots, exhibits distributed sparsity with the sparsity level of  $KQ$ . 238  
This property of  $\mathbf{x}$  inspires us to exploit the SCS theory for the 239  
multiuser signal detection [14]. To further improve the signal detection 240  
performance and to increase the system's throughput, we propose a 241  
joint SM transmission scheme and an SCS-based MUD, which will be 242  
detailed in the following section. 243

### III. SCS-BASED MUD FOR LS-SM-MIMO UL 244

To solve the multiuser signal detection of our UL LS-SM-MIMO 245  
system, we first propose a joint SM transmission scheme to be 246  
employed at the users. Accordingly, an SCS-based low-complexity 247  
MUD is developed at the BS, whereby the distributed sparsity of the 248  
aggregate SM signal and the group sparsity of multiple aggregate SM 249  
signals are exploited. Moreover, the computational complexity of the 250  
proposed SCS-based MUD is discussed. 251

#### A. Joint SM Transmission Scheme at the Users 252

For the  $k$ th user in the  $q$ th time slot, every successive  $J$  CPSC block 253  
is considered as a group, and they share the same spatial constellation 254  
symbol, i.e., 255

$$\begin{aligned} \text{supp}(\mathbf{x}_{k,q}^{(1)}) &= \text{supp}(\mathbf{x}_{k,q}^{(2)}) = \cdots = \text{supp}(\mathbf{x}_{k,q}^{(J)}), \\ &1 \leq k \leq K, 1 \leq q \leq Q \quad (7) \end{aligned}$$

where we introduce the superscript ( $j$ ) to denote the  $j$ th CPSC block, 256  
and  $J$  is typically small, e.g.,  $J = 2$ . In CS theory, the specific signal 257  
structure, where  $\mathbf{x}_{k,q}^{(1)}, \mathbf{x}_{k,q}^{(2)}, \dots, \mathbf{x}_{k,q}^{(J)}$  share a common support, is often 258  
referred to as the *group sparsity*. Similarly, the aggregate SM signals 259  
consisting of the  $K$  users' SM signals also exhibit group sparsity, i.e., 260

$$\text{supp}(\mathbf{x}^{(1)}) = \text{supp}(\mathbf{x}^{(2)}) = \cdots = \text{supp}(\mathbf{x}^{(J)}). \quad (8)$$

Although exhibiting group sparsity may slightly reduce the informa- 261  
tion carried by the spatial constellation symbols, it is also capable of 262

263 reducing the number of the RF chains required according to the SCS  
264 theory, while simultaneously improving the total bit error rate (BER)  
265 of the entire system even with higher UL throughput. This conclusion  
266 will be confirmed by our simulation results.

#### 267 B. SCS-Based MUD at the BS

268 According to (4), the received signals at the BS in the same group  
269 can be expressed as

$$\mathbf{y}^{(j)} = \tilde{\mathbf{H}}^{(j)} \mathbf{x}^{(j)} + \mathbf{w}^{(j)}, \quad 1 \leq j \leq J \quad (9)$$

270 where  $\mathbf{y}^{(j)}$  denotes the received signal in the  $j$ th CPSC block, whereas  
271  $\tilde{\mathbf{H}}^{(j)}$  and  $\mathbf{w}^{(j)}$  are the effective MIMO channel matrix and the AWGN  
272 vector, respectively.

273 The intrinsically distributed sparsity of  $\mathbf{x}^{(j)}$  and the underdeter-  
274 mined nature of (9) inspire us to solve the signal detection problem  
275 based on CS theory, which can efficiently acquire the sparse solutions  
276 to underdetermined linear systems. Moreover, the  $J$  different aggre-  
277 gate SM signals in (9) can be jointly exploited for improving the signal  
278 detection performance due to the group sparsity of  $\{\mathbf{x}^{(j)}\}_{j=1}^J$ . Thus,  
279 by considering both the distributed sparsity and the group sparsity of  
280 the aggregate SM signals, the multiuser signal detection at the BS can  
281 be formulated as the following optimization problem:

$$\begin{aligned} \min_{\{\hat{\mathbf{x}}^{(j)}\}_{j=1}^J} & \sum_{j=1}^J \|\mathbf{y}^{(j)} - \tilde{\mathbf{H}}^{(j)} \hat{\mathbf{x}}^{(j)}\|_2^2 = \min_{\{\hat{\mathbf{x}}_{k,q}^{(j)}\}_{j=1, k=1, q=1}^{J, K, Q}} \\ & \sum_{j=1}^J \|\mathbf{y}^{(j)} - \tilde{\mathbf{H}}^{(j)} \hat{\mathbf{x}}^{(j)}\|_2^2 \\ \text{s.t.} & \|\hat{\mathbf{x}}_{k,q}^{(j)}\|_0 = 1, \quad 1 \leq j \leq J, \quad 1 \leq q \leq Q, \quad 1 \leq k \leq K. \end{aligned} \quad (10)$$

282 Our proposed SCS-based MUD solves the optimization problem (10)  
283 with the aid of two steps. In the first step, we estimate the spatial  
284 constellation symbols, i.e., the indexes of  $K$  users' active AEs in  $J$   
285 successive CPSC blocks. In the second step, we infer the legitimate  
286 signal constellation symbols of the  $K$  users in  $J$  CPSC blocks.

287 *1. Step 1— Estimation of Spatial Constellation Symbols:* We pro-  
288 pose a group subspace pursuit (GSP) algorithm developed from the  
289 classical subspace pursuit (SP) algorithm in [15] to acquire the  
290 sparse solution to the large-scale underdetermined problem (10),  
291 where both the *a priori* sparse information (i.e.,  $\|\mathbf{x}_{k,q}^{(j)}\|_0 = 1$ ) and  
292 the group sparsity of  $\mathbf{x}^{(1)}, \mathbf{x}^{(2)}, \dots, \mathbf{x}^{(J)}$  are exploited for improv-  
293 ing the multiuser signal detection performance. The proposed GSP  
294 algorithm is described in **Algorithm 1**, which estimates SM signal  
295  $\{\hat{\mathbf{x}}_{k,q}^{(j)}\}_{k=1, j=1, q=1}^{K, J, Q}$ . Hence, the estimated spatial constellation symbol  
296 is  $\{\text{supp}(\hat{\mathbf{x}}_{k,q}^{(j)})\}_{k=1, j=1, q=1}^{K, J, Q}$ .

---

#### Algorithm 1 Proposed GSP Algorithm.

---

297 **Input:** Noisy received signals  $\mathbf{y}^{(j)}$  and effective channel matrices  
298  $\tilde{\mathbf{H}}^{(j)}$  for  $1 \leq j \leq J$ .

299 **Output:** Estimated  $\hat{\mathbf{x}}^{(j)} = [(\hat{\mathbf{x}}_1^{(j)})^T (\hat{\mathbf{x}}_2^{(j)})^T, \dots, (\hat{\mathbf{x}}_Q^{(j)})^T]^T$ , where  
300  $\hat{\mathbf{x}}_q^{(j)} = [(\hat{\mathbf{x}}_{1,q}^{(j)})^T (\hat{\mathbf{x}}_{2,q}^{(j)})^T, \dots, (\hat{\mathbf{x}}_{K,q}^{(j)})^T]^T$  for  $1 \leq q \leq Q$ .

301 1:  $\mathbf{r}^{(j)} = \mathbf{y}^{(j)}$  for  $1 \leq j \leq J$ ; {Initialization}

302 2:  $\Omega^0 = \emptyset$ ; {Empty support set}

303 3:  $t = 1$ ; {Iteration index}

4: **repeat** 304  
5:  $\mathbf{a}_{k,q}^{(j)} = (\tilde{\mathbf{H}}_{k,q}^{(j)})^* \mathbf{r}^{(j)}$  for  $1 \leq k \leq K, 1 \leq q \leq Q$ , and  $1 \leq j \leq J$ ; 305  
  {Correlation} 306  
6:  $\tau_{k,q} = \arg \max_{\tau_{k,q}} \sum_{j=1}^J \|\mathbf{a}_{k,q}^{(j)}\|_{\tau_{k,q}}^2$  for  $1 \leq k \leq K,$  307  
   $1 \leq q \leq Q$ ; {Identify support} 308  
7:  $\Gamma = \{\tau_{k,q} + (k-1 + K(q-1))n_t\}_{k=1, q=1}^{K, Q}$ ; {Preliminary 309  
  support set} 310  
8:  $\mathbf{b}^{(j)}|_{\Omega^{t-1} \cup \Gamma} = (\tilde{\mathbf{H}}^{(j)}|_{\Omega^{t-1} \cup \Gamma})^\dagger \mathbf{y}^{(j)}$  for  $1 \leq j \leq J$ ; {Least 311  
  squares} 312  
9:  $\omega_{k,q} = \arg \max_{\omega_{k,q}} \sum_{j=1}^J \|\mathbf{b}_{k,q}^{(j)}\|_{\omega_{k,q}}^2$  for  $1 \leq k \leq K,$  313  
   $1 \leq q \leq Q$ ; {Pruning support set} 314  
10:  $\Omega^t = \{\omega_{k,q} + (k-1 + K(q-1))n_t\}_{k=1, q=1}^{K, Q}$ ; {Final 315  
  support set} 316  
11:  $\mathbf{c}^{(j)}|_{\Omega^t} = (\tilde{\mathbf{H}}^{(j)}|_{\Omega^t})^\dagger \mathbf{y}^{(j)}$  for  $1 \leq j \leq J$ ; {Least squares} 317  
12:  $\mathbf{r}^{(j)} = \mathbf{y}^{(j)} - \tilde{\mathbf{H}}^{(j)} \mathbf{c}^{(j)}$  for  $1 \leq j \leq J$ ; {Compute residual} 318  
13:  $t = t + 1$ ; {Update iteration index} 319  
14: **until**  $\Omega^t = \Omega^{t-1}$  or  $t \geq Q$  320

---

Compared with the classical SP algorithm, the proposed GSP algo- 321  
rithm exploits the distributed sparsity and group sparsity of  $\{\mathbf{x}^{(j)}\}_{j=1}^J$ . 322  
More explicitly,  $\mathbf{x}^{(j)} \in \mathbb{C}^{(KQn_t)}$  consists of the  $KQ$  low-dimensional 323  
sparse vectors  $\mathbf{x}_{k,q}^{(j)} \in \mathbb{C}^{n_t}$ , where each  $\mathbf{x}_{k,q}^{(j)}$  has the known sparsity 324  
level of one, and the aggregate SM signals  $\mathbf{x}^{(1)}, \mathbf{x}^{(2)}, \dots, \mathbf{x}^{(J)}$  exhibit 325  
group sparsity. Specifically, the differences between the proposed GSP 326  
algorithm and the classical SP algorithm lie in the following two 327  
aspects: 1) the identification of the support set including the steps 328  
of the *preliminary support set* and the *final support set* as shown in 329  
**Algorithm 1**; and 2) the joint processing of  $\mathbf{y}^{(1)}, \mathbf{y}^{(2)}, \dots, \mathbf{y}^{(J)}$ . First, 330  
for the support selection, taking the step of the *preliminary support set* 331  
for instance, when selecting the preliminary support set, the classical 332  
SP algorithm selects the support set associated with the first  $KQ$  333  
largest values of the global correlation result  $(\tilde{\mathbf{H}}^{(j)})^* \mathbf{r}^{(j)}$ . By contrast, 334  
the proposed GSP algorithm selects the support set associated with 335  
the largest value from the local correlation result in each  $(\tilde{\mathbf{H}}_{k,q}^{(j)})^* \mathbf{r}^{(j)}$ . 336  
This way, the distributed sparsity of the aggregate SM signal can be ex- 337  
ploited for improved signal detection performance. Second, compared 338  
with the classical SP algorithm, the proposed GSP algorithm jointly 339  
exploits the  $J$  correlated signals having the group sparsity, which can 340  
bring the further improved signal detection performance. 341

It should be noted that even for the special case of  $J = 1$ , i.e., 342  
without using the joint SM transmission scheme, the proposed GSP 343  
algorithm still achieves a better signal detection performance than 344  
the classical SP algorithm when handling the aggregate SM signal, 345  
since the inherently distributed sparsity of the aggregate SM signal is 346  
leveraged to improve the signal detection performance. 347

2. *Step 2— Acquisition of Signal Constellation Symbols:* Following 348  
*Step 1*, we can also acquire a rough estimate of the signal constellation 349  
symbol for each user in each time slot. By searching for the minimum 350  
Euclidean distance between this rough estimate of the signal constel- 351  
lation symbol and the legitimate constellation symbols of  $\mathbb{L}$ , we can 352  
obtain the final estimate of signal constellation symbols. 353

#### C. Computational Complexity 354

The optimal ML signal detector has a prohibitively high com- 355  
putational complexity of  $\mathcal{O}((L \cdot n_t)^{(K \cdot Q)})$  according to (6). The 356  
sphere decoding detectors [10] are indeed capable of reducing the 357  
computational complexity, but they may still suffer from unaffordable 358  
complexity, particularly for large  $K, Q, L$ , and  $n_t$  values. By contrast, 359  
the conventional MMSE-based detector for LS-MIMO and CS-based 360

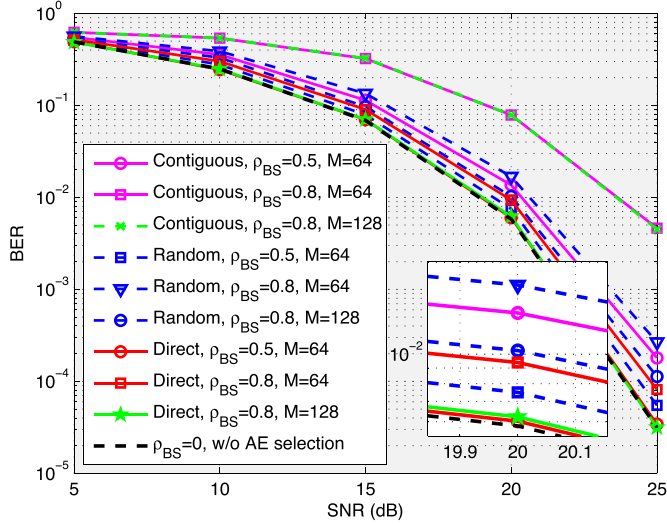


Fig. 2. Total BERs achieved by the proposed SCS-based MUD with different AE selection schemes, where  $K = 8$ ,  $J = 2$ , 64-QAM,  $M_{\text{RF}} = 18$ ,  $n_t = 4$ , and  $\rho_{\text{US}} = 0$  are considered.

361 detector [13] for small-scale SM-MIMO enjoy the low complexity of  
 362  $\mathcal{O}(M_{\text{RF}} \cdot (n_t \cdot Q \cdot K)^2 + (n_t \cdot Q \cdot K)^3)$  and  $\mathcal{O}(2M_{\text{RF}} \cdot (Q \cdot K)^2 +$   
 363  $(Q \cdot K)^3)$ , respectively. For the proposed SCS-based MUD, most  
 364 of the computational requirements are imposed by the least squares  
 365 (LS) operations, which has complexity of  $\mathcal{O}(J \cdot (2M_{\text{RF}} \cdot (Q \cdot K)^2 +$   
 366  $(Q \cdot K)^3))$  [16]. Consequently, the computational complexity per  
 367 CPSC block is  $\mathcal{O}(2M_{\text{RF}} \cdot (Q \cdot K)^2 + (Q \cdot K)^3)$ , since  $J$  successive  
 368 aggregate SM signals are jointly processed. Compared with conven-  
 369 tional signal detectors, the proposed SCS-based MUD benefits from  
 370 substantially lower complexity, and it has similar low complexity as  
 371 the conventional MMSE- and CS-based signal detectors.

372

#### IV. SIMULATION RESULTS

373 A simulation study was carried out to compare the attainable perfor-  
 374 mance of the proposed SCS-based MUD to that of the MMSE-based  
 375 signal detector [4] and to that of the CS-based signal detector [13].  
 376 In the LS-SM-MIMO system considered, the BS used a ULA relying  
 377 on a large number of AEs  $M$ , but a much smaller number of RF  
 378 chains  $M_{\text{RF}}$ , whereas  $K$  users employing  $n_t$  AEs but only a single RF  
 379 chain simultaneously use the CPSC scheme associated with  $P = 8$  and  
 380  $Q = 64$  to transmit the SM signals to the BS. The total BER including  
 381 both the spatial constellation symbols and the signal constellation  
 382 symbols was evaluated.

383 Fig. 2 compares the total BERs achieved by the proposed SCS-based  
 384 MUD with different AE selection schemes, where  $K = 8$ ,  $J = 2$ ,  
 385 64-QAM,  $M_{\text{RF}} = 18$ ,  $n_t = 4$ , and  $\rho_{\text{US}} = 0$  are considered. The con-  
 386 tiguous AE selection scheme implies that we select  $M_{\text{RF}}$  adjacent  
 387 AEs, i.e.,  $\Theta = \{\varphi + m_{\text{RF}}\}_{m_{\text{RF}}=0}^{M_{\text{RF}}-1}$  with  $1 \leq \varphi \leq M - M_{\text{RF}} + 1$ . By  
 388 contrast, in the random AE selection scheme, the elements of  $\Theta$  are  
 389 randomly selected from the set  $\{1, 2, \dots, M\}$ , whereas the direct  
 390 AE selection scheme in [7] has been described in Section II-B.  
 391 Furthermore, the BER achieved by the SCS-based MUD relying on  
 392  $\rho_{\text{BS}} = 0$  is also considered as a performance bound, since the choice  
 393 of  $\rho_{\text{BS}} = 0$  and  $\rho_{\text{US}} = 0$  implies the uncorrelated Rayleigh-fading  
 394 MIMO channels. Observe from Fig. 2 that the direct AE selection  
 395 scheme outperforms the other pair of AE selection schemes. Moreover,  
 396 for a certain AE selection scheme, the BER performance degrades  
 397 when  $M_{\text{RF}}/M$  or  $\rho_{\text{BS}}$  increases. For the direct AE selection scheme,  
 398 the BER performance of  $\rho_{\text{BS}} = 0.8$ ,  $M = 128$  and of  $\rho_{\text{BS}} = 0.5$ ,

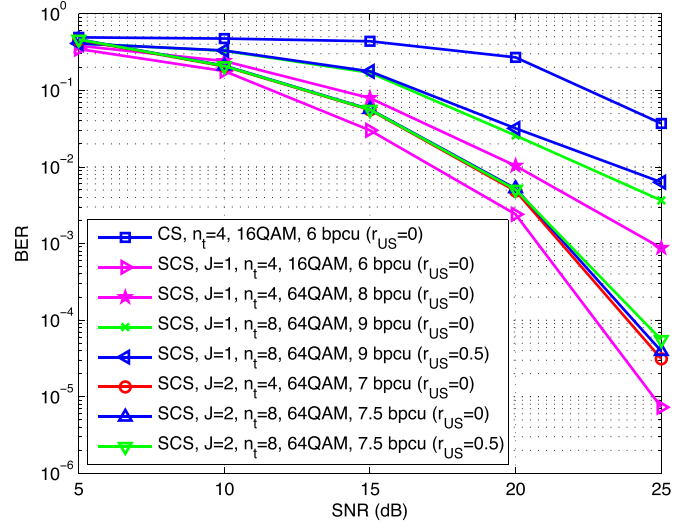


Fig. 3. Total BERs achieved by the CS-based signal detector and the SCS-based MUD against different SNRs in LS-SM-MIMO, where  $K = 8$ ,  $M_{\text{RF}} = 18$ ,  $M = 64$ ,  $\rho_{\text{BS}} = 0.5$ , and the direct AE selection scheme is considered.

$M = 64$  approaches the BER achieved for transmission over uncor- 399  
 400 related Rayleigh-fading MIMO channels, which confirms the near-  
 401 optimal performance of the direct AE selection scheme.

402 Fig. 3 compares the overall BER achieved by the CS-based signal  
 403 detector and by the proposed SCS-based MUD versus the SNR in our  
 404 LS-SM-MIMO context, where  $K = 8$ ,  $M_{\text{RF}} = 18$ ,  $M = 64$ ,  $\rho_{\text{BS}} = 0.5$ ,  
 405 and the direct AE selection scheme is considered. The SCS-based  
 406 MUD outperforms the CS-based signal detector even for  $J = 1$ , since  
 407 the distributed sparsity of the aggregate SM signal is exploited. For the  
 408 SCS-based MUD, the BER performance improves when  $J$  increases,  
 409 albeit this is achieved at the cost of reduced UL throughput. To mitigate  
 410 this impediment, a higher number of AEs can be employed by the users  
 411 for expanding the spatial constellation symbol set constituted by the  
 412 AEs. Specifically, by increasing  $n_t$  from 4 to 8, the UL throughput  
 413 of the SCS-based MUD may be increased, but having more AEs at  
 414 the user results in a higher  $\rho_{\text{US}}$ . When  $n_t$  is increased, the BER  
 415 performance of the SCS-based MUD associated with  $J = 1$  degrades,  
 416 as expected. By contrast, when  $n_t$  is increased, the BER performance  
 417 loss of the SCS-based MUD using  $J = 2$  can be less than 0.2 dB if the  
 418 BER of  $10^{-4}$  is considered, even when a higher  $\rho_{\text{US}}$  associated with a  
 419 higher  $n_t$  is considered.

420 Fig. 4 portrays the BER achieved by the different signal detectors as  
 421 a function of the SNR in the context of the proposed LS-SM-MIMO  
 422 for  $K = 8$ ,  $M_{\text{RF}} = 18$ ,  $M = 64$ ,  $n_t = 4$ ,  $\rho_{\text{BS}} = 0.5$ , and  $\rho_{\text{US}} = 0$ ,  
 423 where the direct AE selection scheme is also considered. In Fig. 4,  
 424 we also characterize the ‘oracle-assisted’ LS-based signal detector  
 425 relying on the assumption that the spatial constellation symbol is  
 426 perfectly known at the BS for the proposed LS-SM-MIMO scheme  
 427 associated with  $J = 2$ , 64-QAM as well as for the MMSE-based  
 428 LS-MIMO detector in conjunction with 64-QAM, where both of them  
 429 only consider the BER of the classic signal constellation symbol. Here,  
 430 we assume that the LS-MIMO arrangement uses the same number  
 431 of RF chains to serve eight single-antenna users communicating  
 432 over uncorrelated Rayleigh-fading channels. The superiority of our  
 433 SCS-based MUD over the MMSE- and CS-based signal detectors  
 434 becomes clear.

435 Moreover, the performance gap between the oracle LS-based signal  
 436 detector associated with 7 bpcu and the proposed SCS-based MUD  
 437 with 7 bpcu is less than 0.5 dB. Note again that the oracle LS-based sig-  
 438 nal detector only considers the BER of the classic signal constellation

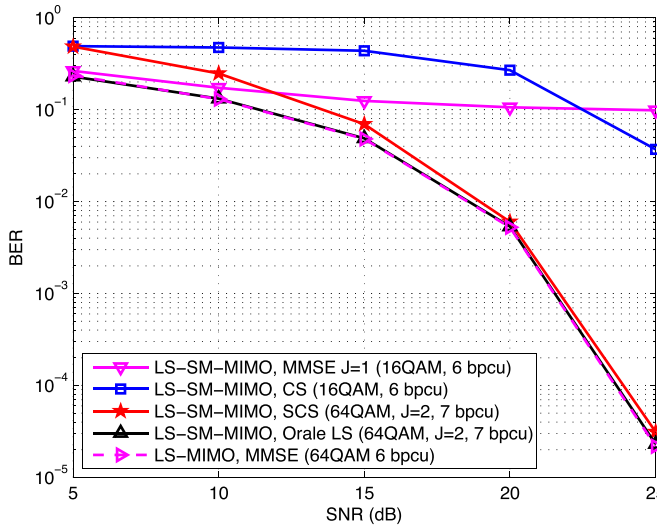


Fig. 4. Total BERs achieved by different signal detectors against different SNRs in the proposed LS-SM-MIMO and conventional LS-MIMO.

439 symbol, whereas the proposed SCS-based MUD considers both the  
 440 spatial and the classic signal constellation symbols. Finally, compared  
 441 with the conventional LS-MIMO using the MMSE-based signal de-  
 442 tector (6 bpcu), our proposed UL LS-SM-MIMO and the associated  
 443 SCS-based MUD (7 bpcu) only suffer from a negligible BER loss,  
 444 which explicitly confirmed the improved UL throughput of the pro-  
 445 posed LS-SM-MIMO scheme.

446

## V. CONCLUSION

447 We have proposed an LS-SM-MIMO scheme for the UL transmis-  
 448 sion. The BS employs a large number of AEs but a much smaller  
 449 number of RF chains, where a simple receive AE selection scheme is  
 450 used for the improved performance. Each user equipped with multiple  
 451 AEs but only a single RF chain uses CPSC to combat multipath chan-  
 452 nels. SM has been adopted for the UL transmission to improve the UL  
 453 throughput. The proposed scheme is particularly suitable for scenarios  
 454 where a large number of low-cost AEs can be accommodated, and  
 455 both power consumption and hardware cost are heavily determined  
 456 by the number of RF chains. Due to the reduced number of RF chains  
 457 at the BS and multiple AEs employed by each user, the UL multiuser  
 458 signal detection is a challenging large-scale underdetermined problem.  
 459 We have proposed a joint SM transmission scheme at the users to  
 460 introduce the group sparsity of multiple aggregate SM signals, and a

matching SCS-based MUD at the BS has been proposed to leverage the  
 461 inherently distributed sparsity of the aggregate SM signal as well as the  
 462 group sparsity of multiple aggregate SM signals for reliable multiuser  
 463 signal detection performance. The proposed SCS-based MUD enjoys  
 464 the low complexity, and our simulation results have demonstrated that  
 465 it performs better than its conventional counterparts with even much  
 466 higher UL throughput. 467

## REFERENCES

- 468
- [1] M. D. Renzo, H. Haas, A. Ghayeb, S. Sugiura, and L. Hanzo, "Spatial  
 469 modulation for generalized MIMO: Challenges, opportunities and  
 470 implementation," *Proc. IEEE*, vol. 102, no. 1, pp. 56–103, Jan. 2014. 471
  - [2] A. Younis, R. Mesleh, M. Di Renzo, and H. Haas, "Generalised spatial  
 472 modulation for large-scale MIMO," in *Proc. EUSIPCO*, Sep. 2014, 473  
 pp. 346–350. 474
  - [3] S. Ganesan, R. Mesleh, H. Haas, C. Ahn, and S. Yun, "On the performance  
 475 of spatial modulation OFDM," in *Proc. 40th Asilomar Conf. Signals, Syst.* 476  
*Comput.*, Oct. 2006, pp. 1825–1829. 477
  - [4] F. Rusek *et al.* "Scaling up MIMO: Opportunities and challenges with  
 478 very large arrays," *IEEE Signal Process. Mag.*, vol. 30, no. 1, pp. 40–60, 479  
 Jan. 2013. 480
  - [5] N. Serafimovski *et al.*, "Practical implementation of spatial modulation,"  
 481 *IEEE Trans. Veh. Technol.*, vol. 62, no. 9, pp. 4511–4523, Nov. 2013. 482
  - [6] P. Som and A. Chockalingam, "Spatial modulation and space shift  
 483 keying in single carrier" in *Proc. IEEE Int. Symp. PIMRC*, Sep. 2012, 484  
 pp. 1062–1067. 485
  - [7] X. Wu, M. Di Renzo, and H. Haas, "Adaptive selection of antennas for  
 486 optimum transmission in spatial modulation," *IEEE Trans. Wireless* 487  
*Commun.*, vol. 14, no. 7, pp. 3630–3641, Jul. 2015. 488
  - [8] S. Narayanan *et al.*, "Multi-user spatial modulation MIMO" in *Proc. IEEE* 489  
*WCNC*, Apr. 2014, pp. 671–676. 490
  - [9] X. Wu, H. Claussen, M. D. Renzo, and H. Haas, "Channel estimation  
 491 for spatial modulation," *IEEE Trans. Commun.*, vol. 62, no. 12, 492  
 pp. 4362–4372, Dec. 2014. 493
  - [10] A. Younis, S. Sinanovic, M. Di Renzo, R. Mesleh, and H. Haas,  
 494 "Generalised sphere decoding for spatial modulation," *IEEE Trans.* 495  
*Commun.*, vol. 61, no. 7, pp. 2805–2815, Jul. 2013. 496
  - [11] W. Liu, N. Wang, M. Jin, and H. Xu, "Denosing detection for the gener-  
 497 alized spatial modulation system using sparse property," *IEEE Commun.* 498  
*Lett.*, vol. 18, no. 1, pp. 22–25, Jan. 2014. 499
  - [12] B. Shim, S. Kwon, and B. Song, "Sparse detection with integer constraint  
 500 using multipath matching pursuit," *IEEE Commun. Lett.*, vol. 18, no. 10, 501  
 pp. 1851–1854, Oct. 2014. 502
  - [13] C. Yu *et al.*, "Compressed sensing detector design for space shift keying  
 503 in MIMO systems," *IEEE Commun. Lett.*, vol. 16, no. 10, pp. 1556–1559, 504  
 Oct. 2012. 505
  - [14] M. F. Duarte and Y. C. Eldar, "Structured compressed sensing: From  
 506 theory to applications," *IEEE Trans. Signal Process.*, vol. 59, no. 9, 507  
 pp. 4053–4085, Sep. 2011. 508
  - [15] W. Dai and O. Milenkovic, "Subspace pursuit for compressive sens-  
 509 ing signal reconstruction," *IEEE Trans. Inf. Theory*, vol. 55, no. 5, 510  
 pp. 2230–2249, May 2009. 511
  - [16] A. Björck, *Numerical Methods for Matrix Computations*. Cham, 512  
 Switzerland: Springer Int. Publ. AG, 2014. 513

## AUTHOR QUERY

NO QUERY.

# Correspondence

## 1 Compressive-Sensing-Based Multiuser Detector for the 2 Large-Scale SM-MIMO Uplink

3 Zhen Gao, Linglong Dai, Zhaocheng Wang, *Senior Member, IEEE*,  
4 Sheng Chen, *Fellow, IEEE*, and Lajos Hanzo, *Fellow, IEEE*

5 **Abstract**—Conventional spatial modulation (SM) is typically consid-  
6 ered for transmission in the downlink of small-scale multiple-input-  
7 multiple-output (MIMO) systems, where a single antenna element (AE) of  
8 a set of, e.g.,  $2^P$  AEs is activated for implicitly conveying  $p$  bits. By contrast,  
9 inspired by the compelling benefits of large-scale MIMO (LS-MIMO)  
10 systems, here, we propose an LS-SM-MIMO scheme for the uplink (UL),  
11 where each user having multiple AEs but only a single radio frequency  
12 (RF) chain invokes SM for increasing the UL throughput. At the same time,  
13 by relying on hundreds of AEs and a small number of RF chains, the base  
14 station (BS) can simultaneously serve multiple users while reducing the  
15 power consumption. Due to the large number of AEs of the UL users and  
16 the comparably small number of RF chains at the BS, the UL multiuser sig-  
17 nal detection becomes a challenging large-scale underdetermined problem.  
18 To solve this problem, we propose a joint SM transmission scheme and  
19 a carefully designed structured compressive sensing (SCS)-based multi-  
20 user detector (MUD) to be used at the users and the BS, respectively.  
21 Additionally, the cyclic-prefix single carrier (CPSC) is used to combat  
22 the multipath channels, and a simple receive AE selection is used for the  
23 improved performance over correlated Rayleigh-fading MIMO channels.  
24 We demonstrate that the aggregate SM signal consisting of multiple UL  
25 users' SM signals of a CPSC block exhibits distributed sparsity. Moreover,  
26 due to the joint SM transmission scheme, aggregate SM signals in the same  
27 transmission group exhibit group sparsity. By exploiting these intrinsically  
28 sparse features, the proposed SCS-based MUD can reliably detect the  
29 resultant SM signals with low complexity. Simulation results demonstrate  
30 that the proposed SCS-based MUD achieves a better signal detection  
31 performance than its counterparts even with higher UL throughput.

32 **Index Terms**—Compressive sensing (CS), large-scale multiple-input-  
33 multiple-output (LS-MIMO), multiuser detector (MUD), spatial modula-  
34 tion (SM).

### 35 I. INTRODUCTION

36 A widely recognized consensus is that fifth-generation (5G) sys-  
37 tems will be capable of providing significant energy efficiency and  
38 system capacity improvements [1], [2]. Promising techniques, such  
39 as large-scale multiple-input-multiple-output (LS-MIMO) and spatial  
40 modulation (SM)-MIMO systems, are considered as potent candidates  
41 for 5G systems [1]–[5]. LS-MIMO employing hundreds of antenna

Manuscript received May 7, 2015; revised October 1, 2015; accepted  
November 14, 2015. This work was supported in part by the International  
Science and Technology Cooperation Program of China under Grant  
2015DFG12760, by the National Natural Science Foundation of China under  
Grant 61571270 and Grant 61201185, by the Beijing Natural Science Founda-  
tion under Grant 4142027, and by the Foundation of Shenzhen government.  
The review of this paper was coordinated by Dr. Y. Xin.

Z. Gao, L. Dai, and Z. Wang are with the Tsinghua National Laboratory for  
Information Science and Technology (TNList), Department of Electronic Engi-  
neering, Tsinghua University, Beijing 100084, China (e-mail: gao-z11@mails.  
tsinghua.edu.cn; daill@mail.tsinghua.edu.cn; zcwang@mail.tsinghua.edu.cn).

S. Chen and L. Hanzo are with the School of Electronics and Computer  
Science, University of Southampton, Southampton SO17 1BJ, U.K. (e-mail:  
sqc@ecs.soton.ac.uk; lh@ecs.soton.ac.uk).

Color versions of one or more of the figures in this paper are available online  
at <http://ieeexplore.ieee.org>.

Digital Object Identifier 10.1109/TVT.2015.2501460

elements (AEs) at the base station (BS) is capable of improving 42  
spectral efficiency by orders of magnitude, but it suffers from the 43  
nonnegligible power consumption and hardware cost due to one spe- 44  
cific radio frequency (RF) chain usually required by every AE [5]. 45  
By using a reduced number of RF chains, the emerging SM-MIMO 46  
activates part of available AEs to transmit extra information in the 47  
spatial domain, and it has attracted much attention due to its high en- 48  
ergy efficiency and reduced hardware cost [5]. However, conventional 49  
SM-MIMO is usually considered in the downlink of small-scale 50  
MIMO systems, and therefore, its achievable capacity is limited. Indi- 51  
vidually, both technologies have their own advantages and drawbacks. 52  
By an effective combination of them, one can envision the win-win 53  
situation. SM-MIMO is attractive for LS-MIMO systems, since the 54  
reduced number of required RF chains in SM-MIMO can reduce the 55  
power consumption and hardware cost in conventional LS-MIMO 56  
systems. Moreover, hundreds of AEs used in LS-MIMO can im- 57  
prove the system throughput of SM-MIMO. Such reciprocity enables 58  
LS-MIMO and SM-MIMO to enjoy the apparent compatibility. 59

In this paper, we propose an LS-SM-MIMO scheme for intrinsi- 60  
cally amalgamating the compelling benefits of both LS-MIMO and 61  
SM-MIMO for the 5G uplink (UL) over frequency-selective fading 62  
channels. In the proposed scheme, each UL user equipped with mul- 63  
tiple AEs but only a single RF chain invokes SM for increasing the 64  
UL throughput, and the cyclic-prefix single-carrier (CPSC) transmis- 65  
sion scheme is adopted to combat the multipath channels [6]. At the 66  
BS, hundreds of AEs but only dozens of RF chains are employed to 67  
simultaneously serve multiple users, and a direct AE selection scheme 68  
is used to improve the system performance over correlated Rayleigh- 69  
fading MIMO channels at the BS [7]. The proposed scheme can 70  
be adopted in conventional LS-MIMO as a specific UL-transmission 71  
mode for reducing the power consumption or, alternatively, for energy- 72  
and cost-efficient LS-SM-MIMO, where joint benefits of efficient AE 73  
selection [7], transmit precoding [8], and channel estimation [9] can 74  
be readily exploited. To sum up, the proposed scheme inherits the 75  
advantages of LS-MIMO and SM-MIMO, while reducing the power 76  
consumption and hardware cost. 77

A challenging problem in the proposed UL LS-SM-MIMO scheme 78  
is how to realize a reliable multiuser detector (MUD) with low com- 79  
plexity. The optimal maximum likelihood (ML) signal detector suffers 80  
from excessive complexity. Conventional sphere decoding detectors 81  
cannot be readily used in multiuser scenarios and may still exhibit high 82  
complexity for LS-SM-MIMO [10]. Existing low-complexity linear 83  
signal detectors, e.g., the minimum mean square error (MMSE)-based 84  
signal detector, perform well for conventional LS-MIMO systems 85  
[4]. However, they are unsuitable for the proposed LS-SM-MIMO 86  
UL transmission, since the large number of transmit AEs of the UL 87  
users and the reduced number of receive RF chains at the BS make 88  
UL multiuser signal detection a large-scale underdetermined/rank- 89  
deficient problem. The authors in [11]–[13] proposed compressive 90  
sensing (CS)-based signal detectors to solve the underdetermined 91  
signal detection problem in SM-MIMO systems, but they only consid- 92  
ered the single-user small-scale SM-MIMO systems in the downlink. 93

Against this background, our new contribution is that we exploit 94  
the specific signal structure in the proposed multiuser LS-SM-MIMO 95  
UL transmission, where each user only activates a single AE in each 96  
time slot. Hence, the SM signal of each UL user is sparse with 97



98 the sparsity level of one, and the aggregate SM signal consisting  
 99 of multiple UL users' SM signals of a CPSC block exhibits certain  
 100 distributed sparsity, which can be beneficially exploited for improving  
 101 the signal detection performance at the BS. Moreover, we propose  
 102 a joint SM transmission scheme for the UL users in conjunction  
 103 with an appropriately structured CS (SCS)-based MUD at the BS.  
 104 The proposed SCS-based MUD is specifically tailored to leverage  
 105 the inherently distributed sparsity of the aggregate SM signal and the  
 106 group sparsity of multiple aggregate SM signals, owing to the joint SM  
 107 transmission scheme for reliable signal detection performance. Our  
 108 simulation results demonstrate that the proposed SCS-based MUD is  
 109 capable of outperforming the conventional detectors even with higher  
 110 UL throughput.

111 The rest of this paper is organized as follows. Section II introduces  
 112 the system model of the proposed LS-SM-MIMO scheme. Section III  
 113 specifies the proposed joint SM transmission and SCS-based MUD.  
 114 Section IV provides our simulation results. Section V concludes this  
 115 paper.

116 Throughout this paper, lowercase and uppercase boldface letters  
 117 denote vectors and matrices, respectively, whereas  $(\cdot)^T$ ,  $(\cdot)^*$ ,  $(\cdot)^\dagger$ , and  
 118  $[\cdot]$  denote the transpose, conjugate transpose, Moore–Penrose matrix  
 119 inversion, and the integer floor operators, respectively. The  $l_0$  and  
 120  $l_2$  norm operations are given by  $\|\cdot\|_0$  and  $\|\cdot\|_2$ , respectively. The  
 121 support set of vector  $\mathbf{x}$  is denoted by  $\text{supp}\{\mathbf{x}\}$ , and  $\mathbf{x}_i$  denotes the  $i$ th  
 122 entry of vector  $\mathbf{x}$ . Additionally,  $\mathbf{x}|_\Gamma$  denotes the entries of  $\mathbf{x}$  defined  
 123 in the set  $\Gamma$ ,  $\Phi|_\Gamma$  denotes the submatrix whose columns comprise the  
 124 columns of  $\Phi$  that are defined in  $\Gamma$ , and  $\Phi)_\Gamma$  denotes the submatrix  
 125 whose rows comprise the rows of  $\Phi$  that are defined in  $\Gamma$ . The  
 126 expectation operator is given by  $E\{\cdot\}$ .  $\text{mod}(x, y) = x - \lfloor x/y \rfloor y$  if  
 127  $y \neq 0$  and  $x - \lfloor x/y \rfloor y \neq 0$ , whereas  $\text{mod}(x, y) = y$  if  $y \neq 0$  and  
 128  $x - \lfloor x/y \rfloor y = 0$ .

## 129 II. SYSTEM MODEL

130 We first introduce the proposed LS-SM-MIMO scheme and then  
 131 focus our attention on the UL transmission with an emphasis on the  
 132 multiuser signal detection.

### 133 A. Proposed Multiuser LS-SM-MIMO Scheme

134 As shown in Fig. 1, we consider the proposed LS-SM-MIMO from  
 135 both the BS side and the user side. For conventional LS-MIMO, the  
 136 number of AEs employed by the BS is equal to the number of its RF  
 137 chains [4]. However, the BS in LS-SM-MIMO, as shown in Fig. 1,  
 138 is equipped with a much smaller number of RF chains  $M_{\text{RF}}$  than  
 139 the total number of AEs  $M$ , i.e., we have  $M_{\text{RF}} \ll M$ . Conventional  
 140 LS-MIMO systems typically assume single-antenna users [4]. By  
 141 contrast, in the proposed scheme, each user is equipped with  $n_t > 1$   
 142 AEs but only a single RF chain, and SM is adopted for the UL  
 143 transmission, where only one of the available AEs is activated for  
 144 data transmission. It has been shown that the main power consumption  
 145 and hardware cost of cellular networks comes from the radio access  
 146 network [1]. Hence, using a reduced number of expensive RF chains  
 147 compared with the total number of AEs at the BS can substantially  
 148 reduce both the power consumption and the hardware cost for the  
 149 operators. Meanwhile, it is feasible to incorporate several AEs and a  
 150 single RF chain in the handsets. The resultant increased degrees of  
 151 freedom in the spatial domain may then be exploited for improving  
 152 the UL throughput. The proposed scheme can be considered as an  
 153 optional UL-transmission mode in conventional LS-MIMO systems,  
 154 where AE selection schemes may be adopted for beneficially selecting  
 155 the most suitable  $M_{\text{RF}}$  AEs at the BS to receive UL SM signals [7].  
 156 Alternatively, it can also be used for the UL of LS-SM-MIMO, when

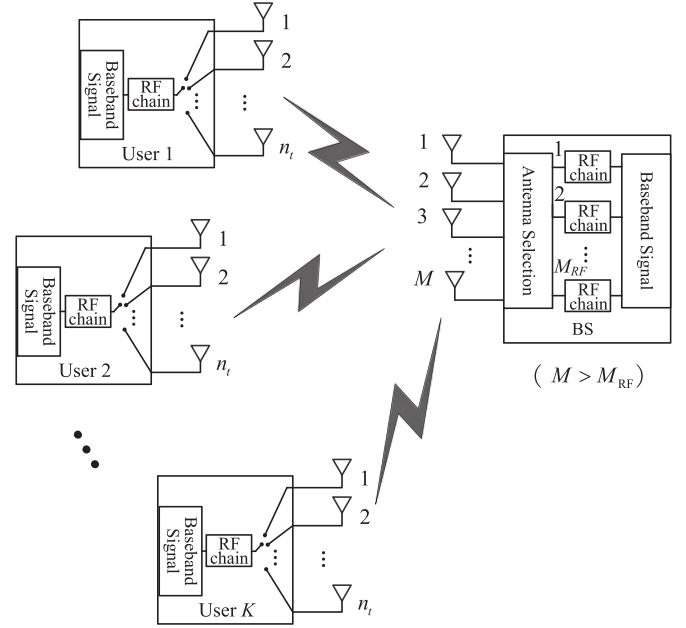


Fig. 1. In the proposed UL LS-SM-MIMO, the BS is equipped with  $M$  AEs and  $M_{\text{RF}}$  RF chains to simultaneously serve  $K$  users, where  $M \gg M_{\text{RF}} > K$ , and each user is equipped with  $n_t > 1$  AEs and one RF chain. By exploiting the improved degree of freedom in the spatial domain, multiple users can simultaneously exploit SM for improving the UL throughput.

157 advantageously combining transmit precoding, receive AE selection,  
 158 and channel estimation [7]–[9].

### 159 B. Uplink Multiuser Transmission

We first consider the generation of SM signals at the users. The SM  
 160 signal  $\mathbf{x}_k = \mathbf{e}_k s_k$  transmitted by the  $k$ th user in a time slot consists  
 161 of two parts: the spatial constellation symbol  $\mathbf{e}_k \in \mathbb{C}^{n_t}$  and the signal  
 162 constellation symbol  $s_k \in \mathbb{C}$ .  $\mathbf{e}_k$  is generated by mapping  $\lfloor \log_2(n_t) \rfloor$   
 163 bits to the index of the active AE, and typically, the user terminal  
 164 employs  $n_t = 2^p$  AEs, where  $p$  is a positive integer. Due to only a  
 165 single RF chain employed at each user, only one entry of  $\mathbf{e}_k$  associated  
 166 with the active AE is equal to one, and the rest of the entries of  $\mathbf{e}_k$  are  
 167 zeros, i.e., we have  
 168

$$\text{supp}(\mathbf{e}_k) \in \mathbb{A}, \quad \|\mathbf{e}_k\|_0 = 1, \quad \|\mathbf{e}_k\|_2 = 1 \quad (1)$$

where  $\mathbb{A} = \{1, 2, \dots, n_t\}$  is the spatial constellation symbol set. The  
 169 signal constellation symbol comes from  $L$ -ary modulation, i.e.,  $s_k \in \mathbb{L}$   
 170 where  $\mathbb{L}$  is the signal constellation symbol set [e.g., 64 quadrature  
 171 amplitude modulation (QAM)] of size  $L$ . Hence, each UL user's SM  
 172 signal carries the information of  $\log_2(L) + \log_2(n_t)$  bits per channel  
 173 use (bpcu), and the overall UL throughput is  $K(\log_2(L) + \log_2(n_t))$   
 174 bpcu. The users rely on the CPSC scheme for transmitting their SM  
 175 signals [6]. Explicitly, each CPSC block consists of a cyclic prefix  
 176 (CP) having the length of  $P - 1$  and the associated data block having  
 177 the length of  $Q$ . Hence, the length of each CPSC block is  $Q + P - 1$ ,  
 178 where this CP is capable of counteracting a dispersive multipath  
 179 channel imposing dispersion over  $P$  samples. The concatenated data  
 180 block consists of  $Q$  successive SM signals.  
 181

At the receiver, due to the reduced number of RF chains at the BS,  
 182 only  $M_{\text{RF}}$  receive AEs can be exploited to receive signals, where exist-  
 183 ing receive AE selection schemes can be adopted to preselect  $M_{\text{RF}}$  re-  
 184 ceive AEs for achieving an improved signal detection performance [7].  
 185 Since the BS can serve  $K$  users simultaneously, after the removal of 186

187 the CP, the received signal  $\mathbf{y}_q \in \mathbb{C}^{M_{\text{RF}}}$  for  $1 \leq q \leq Q$  of the  $q$ th time  
188 slot of a specific CPSC block can be expressed as

$$\begin{aligned} \mathbf{y}_q &= \sum_{k=1}^K \mathbf{y}_{k,q} + \mathbf{w}_q = \sum_{p=0}^{P-1} \sum_{k=1}^K \mathbf{H}_{k,p} \Theta \mathbf{x}_k, \text{ mod } (q-p, Q) \\ &+ \mathbf{w}_q = \sum_{p=0}^{P-1} \sum_{k=1}^K \tilde{\mathbf{H}}_{k,p} \mathbf{x}_k, \text{ mod } (q-p, Q) + \mathbf{w}_q \end{aligned} \quad (2)$$

189 where  $\mathbf{H}_{k,p} \in \mathbb{C}^{M \times n_t}$  is the  $k$ th user's MIMO channel matrix for the  
190  $p$ th multipath component, i.e.,  $\mathbf{H}_{k,p} \Theta = \tilde{\mathbf{H}}_{k,p} \in \mathbb{C}^{M_{\text{RF}} \times n_t}$ ; the set  
191  $\Theta$  is determined by the AE selection scheme used; the elements of  
192  $\Theta$  having the cardinality of  $M_{\text{RF}}$  are uniquely selected from the set  
193  $\{1, 2, \dots, M\}$ ;  $\mathbf{x}_{k,q}$  has one nonzero entry; and  $\mathbf{w}_q \in \mathbb{C}^{M_{\text{RF}}}$  is the  
194 additive white Gaussian noise (AWGN) vector with entries obeying  
195 the independent and identically distributed (i.i.d.) circularly symmet-  
196 ric complex Gaussian distribution with zero mean and a variance  
197 of  $\sigma_w^2/2$  per dimension, which is denoted by  $\mathcal{CN}(0, \sigma_w^2)$ .  $\mathbf{H}_{k,p} =$   
198  $\mathbf{R}_{\text{BS}}^{1/2} \tilde{\mathbf{H}}_{k,p} \mathbf{R}_{\text{US}}^{1/2}$ , the entries of  $\tilde{\mathbf{H}}_{k,p}$  obey the i.i.d.  $\mathcal{CN}(0, 1)$ , and  
199  $\mathbf{R}_{\text{US}}$  with the correlation coefficient  $\rho_{\text{US}}$  and  $\mathbf{R}_{\text{BS}}$  with the correlation  
200 coefficient  $\rho_{\text{BS}}$  are correlation matrices at the users and the BS,  
201 respectively. The specific element of the  $m$ th row and the  $n$ th column  
202 of  $\mathbf{R}_{\text{BS}}$  ( $\mathbf{R}_{\text{US}}$ ) is  $\rho_{\text{BS}}^{|m-n|}$  ( $\rho_{\text{US}}^{|m-n|}$ ). For correlated Rayleigh-fading  
203 MIMO channels, the specific  $\Theta$  or receive AE selection scheme has  
204 an impact on the attainable system performance. In this paper, the  
205 direct AE selection scheme is used for maximizing the minimum  
206 geometric distance between any pair of the selected AEs [7]. For  
207 uniform linear arrays (ULAs),  $\Theta = \{\varphi + m_{\text{RF}} \lfloor M/M_{\text{RF}} \rfloor\}_{m_{\text{RF}}=0}^{M_{\text{RF}}-1}$   
208 with  $1 \leq \varphi \leq \lfloor M/M_{\text{RF}} \rfloor - 1$ . Then, (2) can be further expressed as

$$\mathbf{y}_q = \sum_{p=0}^{P-1} \tilde{\mathbf{H}}_p \mathbf{x} \text{ mod } (q-p, Q) + \mathbf{w}_q \quad (3)$$

209 by defining  $\tilde{\mathbf{H}}_p = [\tilde{\mathbf{H}}_{1,p}, \tilde{\mathbf{H}}_{2,p}, \dots, \tilde{\mathbf{H}}_{K,p}] \in \mathbb{C}^{M_{\text{RF}} \times (n_t K)}$  and  
210  $\mathbf{x}_q = [(\mathbf{x}_{1,q})^T, (\mathbf{x}_{2,q})^T, \dots, (\mathbf{x}_{K,q})^T]^T \in \mathbb{C}^{(n_t K)}$ . By considering  
211 the  $Q$  SM signals of a specific CPSC block, we arrive at

$$\mathbf{y} = \tilde{\mathbf{H}} \mathbf{x} + \mathbf{w} \quad (4)$$

212 where  $\mathbf{y} = [(\mathbf{y}_1)^T, (\mathbf{y}_2)^T, \dots, (\mathbf{y}_Q)^T]^T \in (\mathbb{C}^{M_{\text{RF}} Q})$ , the aggregate  
213 SM signal  $\mathbf{x} = [(\mathbf{x}_1)^T, (\mathbf{x}_2)^T, \dots, (\mathbf{x}_Q)^T]^T \in (\mathbb{C}^{(K n_t Q)})$ ,  $\mathbf{w} =$   
214  $[(\mathbf{w}_1)^T, (\mathbf{w}_2)^T, \dots, (\mathbf{w}_Q)^T]^T$ , and

$$\tilde{\mathbf{H}} = \begin{bmatrix} \tilde{\mathbf{H}}_0 & \mathbf{0} & \mathbf{0} & \cdots & \tilde{\mathbf{H}}_2 & \tilde{\mathbf{H}}_1 \\ \tilde{\mathbf{H}}_1 & \tilde{\mathbf{H}}_0 & \mathbf{0} & \cdots & \vdots & \tilde{\mathbf{H}}_2 \\ \vdots & \tilde{\mathbf{H}}_1 & \tilde{\mathbf{H}}_0 & \cdots & \tilde{\mathbf{H}}_{P-1} & \vdots \\ \tilde{\mathbf{H}}_{P-1} & \vdots & \tilde{\mathbf{H}}_1 & \cdots & \mathbf{0} & \tilde{\mathbf{H}}_{P-1} \\ \mathbf{0} & \tilde{\mathbf{H}}_{P-1} & \vdots & \vdots & \vdots & \mathbf{0} \\ \vdots & \mathbf{0} & \tilde{\mathbf{H}}_{P-1} & \vdots & \vdots & \vdots \\ \vdots & \vdots & \mathbf{0} & \vdots & \mathbf{0} & \vdots \\ \vdots & \vdots & \vdots & \vdots & \tilde{\mathbf{H}}_0 & \mathbf{0} \\ \mathbf{0} & \mathbf{0} & \mathbf{0} & \cdots & \tilde{\mathbf{H}}_1 & \tilde{\mathbf{H}}_0 \end{bmatrix}. \quad (5)$$

215 The signal-to-noise ratio (SNR) at the receiver is defined by  $\text{SNR} =$   
216  $E\{\|\tilde{\mathbf{H}} \mathbf{x}\|_2^2\} / E\{\|\mathbf{w}\|_2^2\}$ .

The optimal signal detector for (4) relies on the ML algorithm, i.e., 217

$$\begin{aligned} \min_{\tilde{\mathbf{x}}} \|\mathbf{y} - \tilde{\mathbf{H}} \tilde{\mathbf{x}}\|_2 &= \min_{\{\tilde{\mathbf{x}}_{k,q}\}_{k=1, q=1}^{K, Q}} \|\mathbf{y} - \tilde{\mathbf{H}} \tilde{\mathbf{x}}\|_2 \\ \text{s.t. } \text{supp}(\tilde{\mathbf{x}}_{k,q}) &\in \mathbb{A}, \tilde{\mathbf{x}}_{k,q} \text{supp}(\tilde{\mathbf{x}}_{k,q}) \in \mathbb{L}, 1 \leq k \leq K, 1 \leq q \leq Q \end{aligned} \quad (6)$$

whose complexity exponentially increases with the number of users, 218  
since the size of the search set for the ML detector is  $(n_t \cdot L)^{KQ}$ . 219  
This excessive complexity can be unaffordable in practice. To reduce 220  
the complexity, near-optimal sphere decoding detectors have been 221  
proposed [10], but their complexity may still remain high, particularly 222  
for the systems supporting large  $K$ ,  $Q$ ,  $n_t$ , and  $L$  [11]. In conventional 223  
LS-MIMO systems, low-complexity linear signal detectors (e.g., the 224  
MMSE-based signal detector) have been shown to be near optimal 225  
since  $M = M_{\text{RF}} \gg K$  and  $n_t = 1$  make multiuser signal detection 226  
an *overdetermined* problem [4]. However, in the proposed scheme, we 227  
have  $M_{\text{RF}} < K n_t$ . Hence, the multiuser signal detection problem (6) 228  
represents a large-scale *underdetermined* problem. Consequently, the 229  
conventional linear signal detectors perform poorly in the proposed 230  
LS-SM-MIMO [11]. By exploiting the sparsity of SM signals, the 231  
authors in [11]–[13] have proposed the concept of CS-based signal 232  
detectors for the downlink of small-scale SM-MIMO operating in a 233  
single-user scenario. However, these signal detectors are unsuitable 234  
for the proposed multiuser scenarios. Observe from (1) that  $\mathbf{x}_{k,q}$  is 235  
a sparse signal having a sparsity level of one. Hence, the aggregate 236  
SM signal  $\mathbf{x}$ , which consists of multiple users' SM signals in  $Q$  237  
time slots, exhibits distributed sparsity with the sparsity level of  $KQ$ . 238  
This property of  $\mathbf{x}$  inspires us to exploit the SCS theory for the 239  
multiuser signal detection [14]. To further improve the signal detection 240  
performance and to increase the system's throughput, we propose a 241  
joint SM transmission scheme and an SCS-based MUD, which will be 242  
detailed in the following section. 243

### III. SCS-BASED MUD FOR LS-SM-MIMO UL 244

To solve the multiuser signal detection of our UL LS-SM-MIMO 245  
system, we first propose a joint SM transmission scheme to be 246  
employed at the users. Accordingly, an SCS-based low-complexity 247  
MUD is developed at the BS, whereby the distributed sparsity of the 248  
aggregate SM signal and the group sparsity of multiple aggregate SM 249  
signals are exploited. Moreover, the computational complexity of the 250  
proposed SCS-based MUD is discussed. 251

#### A. Joint SM Transmission Scheme at the Users 252

For the  $k$ th user in the  $q$ th time slot, every successive  $J$  CPSC block 253  
is considered as a group, and they share the same spatial constellation 254  
symbol, i.e., 255

$$\begin{aligned} \text{supp}(\mathbf{x}_{k,q}^{(1)}) &= \text{supp}(\mathbf{x}_{k,q}^{(2)}) = \cdots = \text{supp}(\mathbf{x}_{k,q}^{(J)}), \\ &1 \leq k \leq K, 1 \leq q \leq Q \end{aligned} \quad (7)$$

where we introduce the superscript ( $j$ ) to denote the  $j$ th CPSC block, 256  
and  $J$  is typically small, e.g.,  $J = 2$ . In CS theory, the specific signal 257  
structure, where  $\mathbf{x}_{k,q}^{(1)}, \mathbf{x}_{k,q}^{(2)}, \dots, \mathbf{x}_{k,q}^{(J)}$  share a common support, is often 258  
referred to as the *group sparsity*. Similarly, the aggregate SM signals 259  
consisting of the  $K$  users' SM signals also exhibit group sparsity, i.e., 260

$$\text{supp}(\mathbf{x}^{(1)}) = \text{supp}(\mathbf{x}^{(2)}) = \cdots = \text{supp}(\mathbf{x}^{(J)}). \quad (8)$$

Although exhibiting group sparsity may slightly reduce the informa- 261  
tion carried by the spatial constellation symbols, it is also capable of 262

263 reducing the number of the RF chains required according to the SCS  
264 theory, while simultaneously improving the total bit error rate (BER)  
265 of the entire system even with higher UL throughput. This conclusion  
266 will be confirmed by our simulation results.

#### 267 B. SCS-Based MUD at the BS

268 According to (4), the received signals at the BS in the same group  
269 can be expressed as

$$\mathbf{y}^{(j)} = \tilde{\mathbf{H}}^{(j)} \mathbf{x}^{(j)} + \mathbf{w}^{(j)}, \quad 1 \leq j \leq J \quad (9)$$

270 where  $\mathbf{y}^{(j)}$  denotes the received signal in the  $j$ th CPSC block, whereas  
271  $\tilde{\mathbf{H}}^{(j)}$  and  $\mathbf{w}^{(j)}$  are the effective MIMO channel matrix and the AWGN  
272 vector, respectively.

273 The intrinsically distributed sparsity of  $\mathbf{x}^{(j)}$  and the underdeter-  
274 mined nature of (9) inspire us to solve the signal detection problem  
275 based on CS theory, which can efficiently acquire the sparse solutions  
276 to underdetermined linear systems. Moreover, the  $J$  different aggre-  
277 gate SM signals in (9) can be jointly exploited for improving the signal  
278 detection performance due to the group sparsity of  $\{\mathbf{x}^{(j)}\}_{j=1}^J$ . Thus,  
279 by considering both the distributed sparsity and the group sparsity of  
280 the aggregate SM signals, the multiuser signal detection at the BS can  
281 be formulated as the following optimization problem:

$$\begin{aligned} \min_{\{\hat{\mathbf{x}}^{(j)}\}_{j=1}^J} & \sum_{j=1}^J \|\mathbf{y}^{(j)} - \tilde{\mathbf{H}}^{(j)} \hat{\mathbf{x}}^{(j)}\|_2^2 = \min_{\{\hat{\mathbf{x}}_{k,q}^{(j)}\}_{j=1, k=1, q=1}^{J, K, Q}} \\ & \sum_{j=1}^J \|\mathbf{y}^{(j)} - \tilde{\mathbf{H}}^{(j)} \hat{\mathbf{x}}^{(j)}\|_2^2 \\ \text{s.t.} & \quad \|\hat{\mathbf{x}}_{k,q}^{(j)}\|_0 = 1, \quad 1 \leq j \leq J, \quad 1 \leq q \leq Q, \quad 1 \leq k \leq K. \end{aligned} \quad (10)$$

282 Our proposed SCS-based MUD solves the optimization problem (10)  
283 with the aid of two steps. In the first step, we estimate the spatial  
284 constellation symbols, i.e., the indexes of  $K$  users' active AEs in  $J$   
285 successive CPSC blocks. In the second step, we infer the legitimate  
286 signal constellation symbols of the  $K$  users in  $J$  CPSC blocks.

287 *1. Step 1— Estimation of Spatial Constellation Symbols:* We pro-  
288 pose a group subspace pursuit (GSP) algorithm developed from the  
289 classical subspace pursuit (SP) algorithm in [15] to acquire the  
290 sparse solution to the large-scale underdetermined problem (10),  
291 where both the *a priori* sparse information (i.e.,  $\|\mathbf{x}_{k,q}^{(j)}\|_0 = 1$ ) and  
292 the group sparsity of  $\mathbf{x}^{(1)}, \mathbf{x}^{(2)}, \dots, \mathbf{x}^{(J)}$  are exploited for improv-  
293 ing the multiuser signal detection performance. The proposed GSP  
294 algorithm is described in **Algorithm 1**, which estimates SM signal  
295  $\{\hat{\mathbf{x}}_{k,q}^{(j)}\}_{k=1, j=1, q=1}^{K, J, Q}$ . Hence, the estimated spatial constellation symbol  
296 is  $\{\text{supp}(\hat{\mathbf{x}}_{k,q}^{(j)})\}_{k=1, j=1, q=1}^{K, J, Q}$ .

---

#### Algorithm 1 Proposed GSP Algorithm.

---

297 **Input:** Noisy received signals  $\mathbf{y}^{(j)}$  and effective channel matrices  
298  $\tilde{\mathbf{H}}^{(j)}$  for  $1 \leq j \leq J$ .

299 **Output:** Estimated  $\hat{\mathbf{x}}^{(j)} = [(\hat{\mathbf{x}}_1^{(j)})^T (\hat{\mathbf{x}}_2^{(j)})^T, \dots, (\hat{\mathbf{x}}_Q^{(j)})^T]^T$ , where  
300  $\hat{\mathbf{x}}_q^{(j)} = [(\hat{\mathbf{x}}_{1,q}^{(j)})^T (\hat{\mathbf{x}}_{2,q}^{(j)})^T, \dots, (\hat{\mathbf{x}}_{K,q}^{(j)})^T]^T$  for  $1 \leq q \leq Q$ .

301 1:  $\mathbf{r}^{(j)} = \mathbf{y}^{(j)}$  for  $1 \leq j \leq J$ ; {Initialization}

302 2:  $\Omega^0 = \emptyset$ ; {Empty support set}

303 3:  $t = 1$ ; {Iteration index}

4: **repeat** 304  
5:  $\mathbf{a}_{k,q}^{(j)} = (\tilde{\mathbf{H}}_{k,q}^{(j)})^* \mathbf{r}^{(j)}$  for  $1 \leq k \leq K, 1 \leq q \leq Q$ , and  $1 \leq j \leq J$ ; 305  
  {Correlation} 306  
6:  $\tau_{k,q} = \arg \max_{\tau_{k,q}} \sum_{j=1}^J \|\mathbf{a}_{k,q}^{(j)}\|_{\tau_{k,q}}^2$  for  $1 \leq k \leq K,$  307  
   $1 \leq q \leq Q$ ; {Identify support} 308  
7:  $\Gamma = \{\tau_{k,q} + (k-1 + K(q-1))n_t\}_{k=1, q=1}^{K, Q}$ ; {Preliminary 309  
  support set} 310  
8:  $\mathbf{b}^{(j)}|_{\Omega^{t-1} \cup \Gamma} = (\tilde{\mathbf{H}}^{(j)}|_{\Omega^{t-1} \cup \Gamma})^\dagger \mathbf{y}^{(j)}$  for  $1 \leq j \leq J$ ; {Least 311  
  squares} 312  
9:  $\omega_{k,q} = \arg \max_{\omega_{k,q}} \sum_{j=1}^J \|\mathbf{b}_{k,q}^{(j)}\|_{\omega_{k,q}}^2$  for  $1 \leq k \leq K,$  313  
   $1 \leq q \leq Q$ ; {Pruning support set} 314  
10:  $\Omega^t = \{\omega_{k,q} + (k-1 + K(q-1))n_t\}_{k=1, q=1}^{K, Q}$ ; {Final 315  
  support set} 316  
11:  $\mathbf{c}^{(j)}|_{\Omega^t} = (\tilde{\mathbf{H}}^{(j)}|_{\Omega^t})^\dagger \mathbf{y}^{(j)}$  for  $1 \leq j \leq J$ ; {Least squares} 317  
12:  $\mathbf{r}^{(j)} = \mathbf{y}^{(j)} - \tilde{\mathbf{H}}^{(j)} \mathbf{c}^{(j)}$  for  $1 \leq j \leq J$ ; {Compute residual} 318  
13:  $t = t + 1$ ; {Update iteration index} 319  
14: **until**  $\Omega^t = \Omega^{t-1}$  or  $t \geq Q$  320

---

Compared with the classical SP algorithm, the proposed GSP algo- 321  
rithm exploits the distributed sparsity and group sparsity of  $\{\mathbf{x}^{(j)}\}_{j=1}^J$ . 322  
More explicitly,  $\mathbf{x}^{(j)} \in \mathbb{C}^{(KQn_t)}$  consists of the  $KQ$  low-dimensional 323  
sparse vectors  $\mathbf{x}_{k,q}^{(j)} \in \mathbb{C}^{n_t}$ , where each  $\mathbf{x}_{k,q}^{(j)}$  has the known sparsity 324  
level of one, and the aggregate SM signals  $\mathbf{x}^{(1)}, \mathbf{x}^{(2)}, \dots, \mathbf{x}^{(J)}$  exhibit 325  
group sparsity. Specifically, the differences between the proposed GSP 326  
algorithm and the classical SP algorithm lie in the following two 327  
aspects: 1) the identification of the support set including the steps 328  
of the *preliminary support set* and the *final support set* as shown in 329  
**Algorithm 1**; and 2) the joint processing of  $\mathbf{y}^{(1)}, \mathbf{y}^{(2)}, \dots, \mathbf{y}^{(J)}$ . First, 330  
for the support selection, taking the step of the *preliminary support set* 331  
for instance, when selecting the preliminary support set, the classical 332  
SP algorithm selects the support set associated with the first  $KQ$  333  
largest values of the global correlation result  $(\tilde{\mathbf{H}}^{(j)})^* \mathbf{r}^{(j)}$ . By contrast, 334  
the proposed GSP algorithm selects the support set associated with 335  
the largest value from the local correlation result in each  $(\tilde{\mathbf{H}}_{k,q}^{(j)})^* \mathbf{r}^{(j)}$ . 336  
This way, the distributed sparsity of the aggregate SM signal can be ex- 337  
ploited for improved signal detection performance. Second, compared 338  
with the classical SP algorithm, the proposed GSP algorithm jointly 339  
exploits the  $J$  correlated signals having the group sparsity, which can 340  
bring the further improved signal detection performance. 341

It should be noted that even for the special case of  $J = 1$ , i.e., 342  
without using the joint SM transmission scheme, the proposed GSP 343  
algorithm still achieves a better signal detection performance than 344  
the classical SP algorithm when handling the aggregate SM signal, 345  
since the inherently distributed sparsity of the aggregate SM signal is 346  
leveraged to improve the signal detection performance. 347

2. *Step 2— Acquisition of Signal Constellation Symbols:* Following 348  
*Step 1*, we can also acquire a rough estimate of the signal constellation 349  
symbol for each user in each time slot. By searching for the minimum 350  
Euclidean distance between this rough estimate of the signal constel- 351  
lation symbol and the legitimate constellation symbols of  $\mathbb{L}$ , we can 352  
obtain the final estimate of signal constellation symbols. 353

#### C. Computational Complexity 354

The optimal ML signal detector has a prohibitively high com- 355  
putational complexity of  $\mathcal{O}((L \cdot n_t)^{(K \cdot Q)})$  according to (6). The 356  
sphere decoding detectors [10] are indeed capable of reducing the 357  
computational complexity, but they may still suffer from unaffordable 358  
complexity, particularly for large  $K, Q, L$ , and  $n_t$  values. By contrast, 359  
the conventional MMSE-based detector for LS-MIMO and CS-based 360

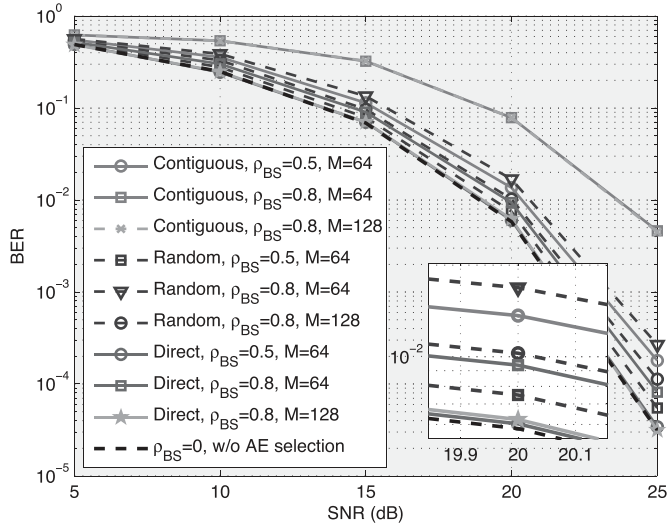


Fig. 2. Total BERs achieved by the proposed SCS-based MUD with different AE selection schemes, where  $K = 8$ ,  $J = 2$ , 64-QAM,  $M_{\text{RF}} = 18$ ,  $n_t = 4$ , and  $\rho_{\text{US}} = 0$  are considered.

361 detector [13] for small-scale SM-MIMO enjoy the low complexity of  
 362  $\mathcal{O}(M_{\text{RF}} \cdot (n_t \cdot Q \cdot K)^2 + (n_t \cdot Q \cdot K)^3)$  and  $\mathcal{O}(2M_{\text{RF}} \cdot (Q \cdot K)^2 +$   
 363  $(Q \cdot K)^3)$ , respectively. For the proposed SCS-based MUD, most  
 364 of the computational requirements are imposed by the least squares  
 365 (LS) operations, which has complexity of  $\mathcal{O}(J \cdot (2M_{\text{RF}} \cdot (Q \cdot K)^2 +$   
 366  $(Q \cdot K)^3))$  [16]. Consequently, the computational complexity per  
 367 CPSC block is  $\mathcal{O}(2M_{\text{RF}} \cdot (Q \cdot K)^2 + (Q \cdot K)^3)$ , since  $J$  successive  
 368 aggregate SM signals are jointly processed. Compared with conven-  
 369 tional signal detectors, the proposed SCS-based MUD benefits from  
 370 substantially lower complexity, and it has similar low complexity as  
 371 the conventional MMSE- and CS-based signal detectors.

372

#### IV. SIMULATION RESULTS

373 A simulation study was carried out to compare the attainable perfor-  
 374 mance of the proposed SCS-based MUD to that of the MMSE-based  
 375 signal detector [4] and to that of the CS-based signal detector [13].  
 376 In the LS-SM-MIMO system considered, the BS used a ULA relying  
 377 on a large number of AEs  $M$ , but a much smaller number of RF  
 378 chains  $M_{\text{RF}}$ , whereas  $K$  users employing  $n_t$  AEs but only a single RF  
 379 chain simultaneously use the CPSC scheme associated with  $P = 8$  and  
 380  $Q = 64$  to transmit the SM signals to the BS. The total BER including  
 381 both the spatial constellation symbols and the signal constellation  
 382 symbols was evaluated.

383 Fig. 2 compares the total BERs achieved by the proposed SCS-based  
 384 MUD with different AE selection schemes, where  $K = 8$ ,  $J = 2$ ,  
 385 64-QAM,  $M_{\text{RF}} = 18$ ,  $n_t = 4$ , and  $\rho_{\text{US}} = 0$  are considered. The con-  
 386 tiguous AE selection scheme implies that we select  $M_{\text{RF}}$  adjacent  
 387 AEs, i.e.,  $\Theta = \{\varphi + m_{\text{RF}}\}_{m_{\text{RF}}=0}^{M_{\text{RF}}-1}$  with  $1 \leq \varphi \leq M - M_{\text{RF}} + 1$ . By  
 388 contrast, in the random AE selection scheme, the elements of  $\Theta$  are  
 389 randomly selected from the set  $\{1, 2, \dots, M\}$ , whereas the direct  
 390 AE selection scheme in [7] has been described in Section II-B.  
 391 Furthermore, the BER achieved by the SCS-based MUD relying on  
 392  $\rho_{\text{BS}} = 0$  is also considered as a performance bound, since the choice  
 393 of  $\rho_{\text{BS}} = 0$  and  $\rho_{\text{US}} = 0$  implies the uncorrelated Rayleigh-fading  
 394 MIMO channels. Observe from Fig. 2 that the direct AE selection  
 395 scheme outperforms the other pair of AE selection schemes. Moreover,  
 396 for a certain AE selection scheme, the BER performance degrades  
 397 when  $M_{\text{RF}}/M$  or  $\rho_{\text{BS}}$  increases. For the direct AE selection scheme,  
 398 the BER performance of  $\rho_{\text{BS}} = 0.8$ ,  $M = 128$  and of  $\rho_{\text{BS}} = 0.5$ ,

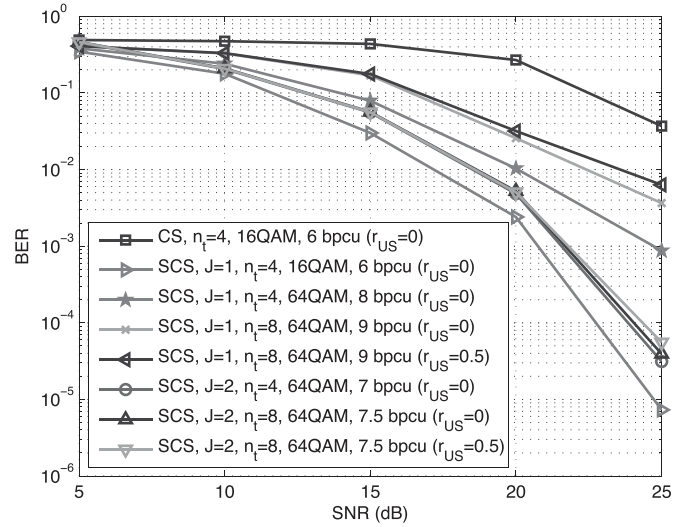


Fig. 3. Total BERs achieved by the CS-based signal detector and the SCS-based MUD against different SNRs in LS-SM-MIMO, where  $K = 8$ ,  $M_{\text{RF}} = 18$ ,  $M = 64$ ,  $\rho_{\text{BS}} = 0.5$ , and the direct AE selection scheme is considered.

$M = 64$  approaches the BER achieved for transmission over uncor- 399  
 400 related Rayleigh-fading MIMO channels, which confirms the near-  
 401 optimal performance of the direct AE selection scheme.

402 Fig. 3 compares the overall BER achieved by the CS-based signal  
 403 detector and by the proposed SCS-based MUD versus the SNR in our  
 404 LS-SM-MIMO context, where  $K = 8$ ,  $M_{\text{RF}} = 18$ ,  $M = 64$ ,  $\rho_{\text{BS}} = 0.5$ ,  
 405 and the direct AE selection scheme is considered. The SCS-based  
 406 MUD outperforms the CS-based signal detector even for  $J = 1$ , since  
 407 the distributed sparsity of the aggregate SM signal is exploited. For the  
 408 SCS-based MUD, the BER performance improves when  $J$  increases,  
 409 albeit this is achieved at the cost of reduced UL throughput. To mitigate  
 410 this impediment, a higher number of AEs can be employed by the users  
 411 for expanding the spatial constellation symbol set constituted by the  
 412 AEs. Specifically, by increasing  $n_t$  from 4 to 8, the UL throughput  
 413 of the SCS-based MUD may be increased, but having more AEs at  
 414 the user results in a higher  $\rho_{\text{US}}$ . When  $n_t$  is increased, the BER  
 415 performance of the SCS-based MUD associated with  $J = 1$  degrades,  
 416 as expected. By contrast, when  $n_t$  is increased, the BER performance  
 417 loss of the SCS-based MUD using  $J = 2$  can be less than 0.2 dB if the  
 418 BER of  $10^{-4}$  is considered, even when a higher  $\rho_{\text{US}}$  associated with a  
 419 higher  $n_t$  is considered.

420 Fig. 4 portrays the BER achieved by the different signal detectors as  
 421 a function of the SNR in the context of the proposed LS-SM-MIMO  
 422 for  $K = 8$ ,  $M_{\text{RF}} = 18$ ,  $M = 64$ ,  $n_t = 4$ ,  $\rho_{\text{BS}} = 0.5$ , and  $\rho_{\text{US}} = 0$ ,  
 423 where the direct AE selection scheme is also considered. In Fig. 4,  
 424 we also characterize the ‘oracle-assisted’ LS-based signal detector  
 425 relying on the assumption that the spatial constellation symbol is  
 426 perfectly known at the BS for the proposed LS-SM-MIMO scheme  
 427 associated with  $J = 2$ , 64-QAM as well as for the MMSE-based  
 428 LS-MIMO detector in conjunction with 64-QAM, where both of them  
 429 only consider the BER of the classic signal constellation symbol. Here,  
 430 we assume that the LS-MIMO arrangement uses the same number  
 431 of RF chains to serve eight single-antenna users communicating  
 432 over uncorrelated Rayleigh-fading channels. The superiority of our  
 433 SCS-based MUD over the MMSE- and CS-based signal detectors  
 434 becomes clear.

435 Moreover, the performance gap between the oracle LS-based signal  
 436 detector associated with 7 bpcu and the proposed SCS-based MUD  
 437 with 7 bpcu is less than 0.5 dB. Note again that the oracle LS-based sig-  
 438 nal detector only considers the BER of the classic signal constellation

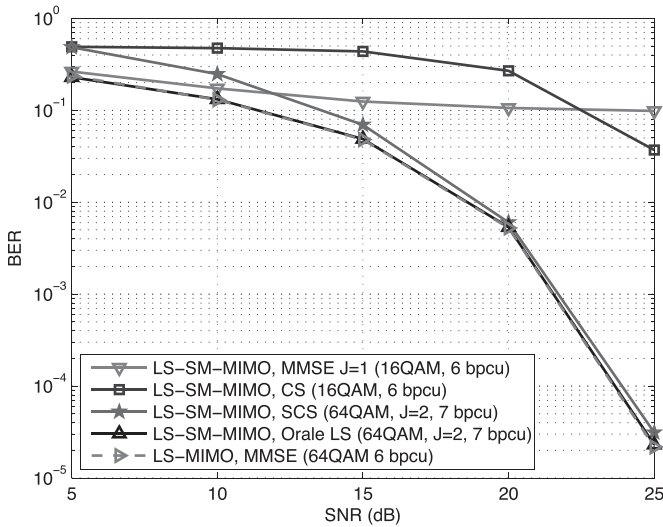


Fig. 4. Total BERs achieved by different signal detectors against different SNRs in the proposed LS-SM-MIMO and conventional LS-MIMO.

439 symbol, whereas the proposed SCS-based MUD considers both the  
 440 spatial and the classic signal constellation symbols. Finally, compared  
 441 with the conventional LS-MIMO using the MMSE-based signal de-  
 442 tector (6 bpcu), our proposed UL LS-SM-MIMO and the associated  
 443 SCS-based MUD (7 bpcu) only suffer from a negligible BER loss,  
 444 which explicitly confirmed the improved UL throughput of the pro-  
 445 posed LS-SM-MIMO scheme.

446

## V. CONCLUSION

447 We have proposed an LS-SM-MIMO scheme for the UL transmis-  
 448 sion. The BS employs a large number of AEs but a much smaller  
 449 number of RF chains, where a simple receive AE selection scheme is  
 450 used for the improved performance. Each user equipped with multiple  
 451 AEs but only a single RF chain uses CPSC to combat multipath chan-  
 452 nels. SM has been adopted for the UL transmission to improve the UL  
 453 throughput. The proposed scheme is particularly suitable for scenarios  
 454 where a large number of low-cost AEs can be accommodated, and  
 455 both power consumption and hardware cost are heavily determined  
 456 by the number of RF chains. Due to the reduced number of RF chains  
 457 at the BS and multiple AEs employed by each user, the UL multiuser  
 458 signal detection is a challenging large-scale underdetermined problem.  
 459 We have proposed a joint SM transmission scheme at the users to  
 460 introduce the group sparsity of multiple aggregate SM signals, and a

matching SCS-based MUD at the BS has been proposed to leverage the  
 461 inherently distributed sparsity of the aggregate SM signal as well as the  
 462 group sparsity of multiple aggregate SM signals for reliable multiuser  
 463 signal detection performance. The proposed SCS-based MUD enjoys  
 464 the low complexity, and our simulation results have demonstrated that  
 465 it performs better than its conventional counterparts with even much  
 466 higher UL throughput. 467

## REFERENCES

- [1] M. D. Renzo, H. Haas, A. Ghayeb, S. Sugiura, and L. Hanzo, "Spatial  
 469 modulation for generalized MIMO: Challenges, opportunities and  
 470 implementation," *Proc. IEEE*, vol. 102, no. 1, pp. 56–103, Jan. 2014. 471
- [2] A. Younis, R. Mesleh, M. Di Renzo, and H. Haas, "Generalised spatial  
 472 modulation for large-scale MIMO," in *Proc. EUSIPCO*, Sep. 2014, 473  
 pp. 346–350. 474
- [3] S. Ganesan, R. Mesleh, H. Haas, C. Ahn, and S. Yun, "On the performance  
 475 of spatial modulation OFDM," in *Proc. 40th Asilomar Conf. Signals, Syst.* 476  
*Comput.*, Oct. 2006, pp. 1825–1829. 477
- [4] F. Rusek *et al.* "Scaling up MIMO: Opportunities and challenges with  
 478 very large arrays," *IEEE Signal Process. Mag.*, vol. 30, no. 1, pp. 40–60, 479  
 Jan. 2013. 480
- [5] N. Serafimovski *et al.*, "Practical implementation of spatial modulation,"  
 481 *IEEE Trans. Veh. Technol.*, vol. 62, no. 9, pp. 4511–4523, Nov. 2013. 482
- [6] P. Som and A. Chockalingam, "Spatial modulation and space shift  
 483 keying in single carrier" in *Proc. IEEE Int. Symp. PIMRC*, Sep. 2012, 484  
 pp. 1062–1067. 485
- [7] X. Wu, M. Di Renzo, and H. Haas, "Adaptive selection of antennas for  
 486 optimum transmission in spatial modulation," *IEEE Trans. Wireless* 487  
*Commun.*, vol. 14, no. 7, pp. 3630–3641, Jul. 2015. 488
- [8] S. Narayanan *et al.*, "Multi-user spatial modulation MIMO" in *Proc. IEEE* 489  
*WCNC*, Apr. 2014, pp. 671–676. 490
- [9] X. Wu, H. Claussen, M. D. Renzo, and H. Haas, "Channel estimation  
 491 for spatial modulation," *IEEE Trans. Commun.*, vol. 62, no. 12, 492  
 pp. 4362–4372, Dec. 2014. 493
- [10] A. Younis, S. Sinanovic, M. Di Renzo, R. Mesleh, and H. Haas,  
 494 "Generalised sphere decoding for spatial modulation," *IEEE Trans.* 495  
*Commun.*, vol. 61, no. 7, pp. 2805–2815, Jul. 2013. 496
- [11] W. Liu, N. Wang, M. Jin, and H. Xu, "Denoising detection for the gener-  
 497 alized spatial modulation system using sparse property," *IEEE Commun.* 498  
*Lett.*, vol. 18, no. 1, pp. 22–25, Jan. 2014. 499
- [12] B. Shim, S. Kwon, and B. Song, "Sparse detection with integer constraint  
 500 using multipath matching pursuit," *IEEE Commun. Lett.*, vol. 18, no. 10, 501  
 pp. 1851–1854, Oct. 2014. 502
- [13] C. Yu *et al.*, "Compressed sensing detector design for space shift keying  
 503 in MIMO systems," *IEEE Commun. Lett.*, vol. 16, no. 10, pp. 1556–1559, 504  
 Oct. 2012. 505
- [14] M. F. Duarte and Y. C. Eldar, "Structured compressed sensing: From  
 506 theory to applications," *IEEE Trans. Signal Process.*, vol. 59, no. 9, 507  
 pp. 4053–4085, Sep. 2011. 508
- [15] W. Dai and O. Milenkovic, "Subspace pursuit for compressive sens-  
 509 ing signal reconstruction," *IEEE Trans. Inf. Theory*, vol. 55, no. 5, 510  
 pp. 2230–2249, May 2009. 511
- [16] A. Björck, *Numerical Methods for Matrix Computations*. Cham, 512  
 Switzerland: Springer Int. Publ. AG, 2014. 513

## AUTHOR QUERY

NO QUERY.